

RESEARCH NOTE

Open Access



# Epidemiological analysis of Lassa fever control using novel mathematical modeling and a dual-dosage vaccination approach

Akeem Olarewaju Yunus<sup>1\*</sup> and Morufu Oyedunsi Olayiwola<sup>1</sup>

## Abstract

Lassa fever is a serious health issue in West Africa that requires deeper understanding in order to be effectively controlled. Compared to conventional integer-order methods, this study presents an improved analysis of disease dynamics, including vaccine efficacy, by utilizing fractional-order models and the Laplace Adomian Decomposition methods. This research highlights the critical role of fractional-order dynamics and vaccination impact in understanding Lassa fever transmission and evaluating control strategies. It employs stability and sensitivity analyses, as well as the next-generation matrix method, to assess the basic reproduction number. The study offers novel insights into the importance of expanded vaccination coverage, setting it apart from previous works. The study demonstrated that preventive strategies, particularly double-dose vaccinations, are extremely efficient in controlling Lassa fever and lowering infection rates. It emphasizes the significance of increasing vaccination efforts to safeguard groups that are susceptible. The findings offer important epidemiological insights, boosting efforts to eradicate the disease and improve public health in West Africa and beyond.

**Keywords** Lassa fever, Vaccination, Stability analysis, Laplace Adomian Decomposition Method, Caputo fractional derivative, Sensitivity analysis

## Introduction

Lassa fever, a severe viral disease first identified in 1969 in Lassa, Nigeria, is primarily transmitted by African rats. It is prevalent in West African nations, including Nigeria, Guinea, Sierra Leone, and Liberia, where its wide spread poses significant health concerns. The disease causes 100,000–300,000 cases and about 5000 deaths annually. Humans are typically infected through contact with contaminated food or objects, such as rat urine and feces. Hospital data from Liberia and Sierra Leone indicate that 10–16% of admitted patients are affected [1–5]. Lassa fever causes symptoms from mild headaches

to severe nasal hemorrhage, with a 6–21 day incubation period. Transmitted by highly contagious rats, it is often fatal, posing a 95% mortality risk for third-trimester pregnancies [6]. Despite global recognition and concerns about its use as a biological weapon, effective mitigation remains absent after five decades. Early containment could have curbed its spread in West Africa. This essay examines the risks, challenges, and recommendations for managing Lassa fever. Ribavirin and protective clothing are essential for treating Lassa fever [7–9]. In order to manage its complicated dynamics and eradicate it in Nigeria, mathematical modeling, public awareness, and education are essential [10, 11]. Significant contributions have been made by researchers [12–15]; for example, [16] devised a nine-compartment model and [17] employed the Laplace transform for modeling.

\*Correspondence:

Akeem Olarewaju Yunus  
akeem.yunus@pgc.uniosun.edu.ng

<sup>1</sup> Department of Mathematical Science, Osun State University, Osogbo, Nigeria



© The Author(s) 2025. **Open Access** This article is licensed under a Creative Commons Attribution-NonCommercial-NoDerivatives 4.0 International License, which permits any non-commercial use, sharing, distribution and reproduction in any medium or format, as long as you give appropriate credit to the original author(s) and the source, provide a link to the Creative Commons licence, and indicate if you modified the licensed material. You do not have permission under this licence to share adapted material derived from this article or parts of it. The images or other third party material in this article are included in the article's Creative Commons licence, unless indicated otherwise in a credit line to the material. If material is not included in the article's Creative Commons licence and your intended use is not permitted by statutory regulation or exceeds the permitted use, you will need to obtain permission directly from the copyright holder. To view a copy of this licence, visit <http://creativecommons.org/licenses/by-nc-nd/4.0/>.

Fractional calculus, which employs arbitrary-order derivatives and integrals, enhances disease modeling by capturing memory effects and providing more accurate predictions. These models aid in predicting disease spread and susceptibility and are widely applied in various fields. Operators such as Atangana-Baleanu, Caputo-Fabrizio, Katugampola, and Caputo-Riemann–Liouville [11, 18–22] enable the analysis of long-range interactions, which is crucial for understanding and controlling infectious diseases. While many studies highlight these applications [15, 21, 23, 24], there is a growing need to apply fractional-order models to real-world scenarios and fractional derivatives have been used for diseases like Lassa fever [25, 26]. The Caputo derivative, with its memory effects, has also enhanced models for COVID-19 immunization and quarantine studies [19]. The Lassa fever outbreak has put a strain on healthcare and lowered life expectancy in Nigeria, a country of 200 million people with an annual growth rate of 2.6%. Between 2021 and February 2022, the fatality rate from Lassa fever decreased from 22.8 to 18.1% [6, 27–30]. Offer a mathematical model to examine the best control measures to lessen the effects of COVID-19 and analyze its spread. To evaluate their efficacy in managing the pandemic, the study takes into account elements including social separation, treatment, and vaccines. Using data from Khyber Pakhtunkhwa, a TB model takes into account environmental factors, treatment, and immunization. For  $R_v < 1$ , a stability study demonstrates disease-free equilibrium; for  $R_v > 1$ , stability is global. The basic reproduction number is  $R_0 = 3.6615$ , and control parameters are identified by sensitivity analysis [31]. This study investigates the UK's monkeypox recurrence with emphasis on vaccination. When a vaccine is administered, disease transmission is predicted by a mathematical model with  $R_2 = 0.48$  and  $R_2 = 0.8$ . High vaccination effectiveness, low waning, and immunizing the infected are essential for effective control, according to sensitivity analysis and simulations [32]. This work uses nonlinear least squares to fit real data and analyze the stability of equilibria in order to model HIV/AIDS dynamics. By calculating the fundamental reproduction number and using sensitivity analysis to pinpoint important factors for disease reduction, it is demonstrated that HIV/AIDS cases can be decreased through prevention [33]. A global health concern, soil-transmitted helminth infections are common in underdeveloped areas. By modeling their transmission, this study finds that an endemic equilibrium (EEP) is stable when  $R_0 > 1$  and a disease-free equilibrium (DFE) is stable when  $R_0 < 1$ . The usefulness of programs that emphasize education and awareness in lowering disease is demonstrated by optimal control measures that focus on hygiene [34]. First and second doses of the vaccine are included in this study's model of COVID-19 dynamics. Stability is determined by

the control reproduction number; a state free of COVID is stable if it is less than one. Sensitivity analysis is used to identify important aspects such as vaccination rates and transmission using data from Malaysia (February 2021–February 2022). Increased immunization and preventive measures successfully lower infection rates, according to simulations [35]. The dynamics of COVID-19 are modeled in this study by including the first and second doses of the vaccine. Stability is determined by the control reproduction number; if it is less than one, a state devoid of COVID is stable. Sensitivity analysis uses data from Malaysia (February 2021–February 2022) to identify important parameters such as vaccination rates and transmission. Infections are efficiently reduced by greater immunization and preventive measures, according to simulations [36]. The dynamics of tuberculosis are modeled in this paper, and stability is examined using Lyapunov functions and  $R_0$ . Using data from Rwanda and Uganda, a Caputo fractional model identifies important infection control factors. According to simulations, increased immunization and treatment lowers the prevalence and burden of tuberculosis [37]. This study uses drug-susceptible and drug-resistant strains of tuberculosis to model the disease and finds a “backward bifurcation,” where both endemic and stable disease-free equilibria coexist when  $R_0 < 1$ . Simulations show that increasing treatment for drug-susceptible patients reduces their incidence but increases drug-resistant TB. When  $R_0 > 1$ , both strains coexist. The results highlight the challenges posed by drug resistance and the importance of mathematical models for tuberculosis control [38]. A mathematical model for analyzing the dynamics of monkeypox is developed in this study, and stability is found when the reproduction number is less than one. It formulates an optimal control problem with four options (treatment, isolation, human-to-human prevention, and prevention of rodent-to-human transmission). The most economical and successful approach, according to simulations, is to stop rodent-to-human transmission [39]. The Laplace Adomian Method and a Caputo fractional order are used in this study to model the transmission of Lassa fever and the effectiveness of double-dose vaccinations. The importance of double-dose vaccines in preventing Lassa fever and enhancing public health is emphasized. These findings can help policymakers assess vaccination programs to develop eradication strategies.

## Preliminaries

Basics of fractional calculus.

**Definition 1** Fractional integration of order  $\nu$  gives

$$\left( \int_{t_0}^{\alpha} h \right) (t) = \frac{1}{\Gamma(\nu)} \int (t-s)^{\nu-1} h(s) ds, \nu \geq 0, t \geq t_0.$$

**Definition 2** Rieman-Liouville derivative of order  $\nu$  gives;

$$D_t^\alpha h(t) = \frac{1}{\Gamma(n-\nu)} \left(\frac{d}{dx}\right)^n \int_a^t (t-u)^{n-\alpha-1} h(u) du$$

**Definition 3** The Caputo fractional gives

$${}^c_0D_t^\nu h(t) = \frac{1}{\Gamma(n-\nu)} \int_a^t (t-u)^{n-\nu-1} h(u) du.$$

**Definition 4** The Adomain polynomials, function  $h(t)$  into a series of polynomial by  $X_0, X_1, \dots, X_n$ .

$$h(t) = h_0 + h_1 + h_2 + \dots \quad \text{as}$$

$$X_n = \frac{1}{n} \frac{d^n}{d\lambda^n} \left[ G(t) \sum_{j=0}^n y_j \lambda^j \right]_{\lambda=0}.$$

### Methods

#### Description of model formulations

This study analyzes the dynamics of Lassa fever, interactions between susceptible and infectious individuals, and immunization all result in a decrease in the transmission rate.

$$\frac{dS(t)}{dt} = \pi + \varepsilon V_1 - \beta SI - (\rho + \mu)S \quad (1)$$

The vaccinated population over time. The first dose provides partial protection, while the rate of entry into the second-dose group depends on the vaccination rate, as shown by below.

$$\frac{dV_1(t)}{dt} = \rho S - (\varepsilon + \kappa + \mu)V_1 \quad (2)$$

The Vaccinated compartment with the second dose, boosting immunity. Flow depends on the vaccination rate and transition from the initial Vaccinated (V) compartment.

$$\frac{dV_2(t)}{dt} = \kappa V_1 - (\psi + \mu)V_2 \quad (3)$$

The Exposed (E) compartment includes those exposed to the virus but not yet contagious, governed by transmission rate and contact with infected individuals.

$$\frac{dE(t)}{dt} = \beta SI - (\gamma + \mu)E \quad (4)$$

The Infected Undetected (U) population includes symptomless individuals, possibly due to immunity or resistance.

$$\frac{dU(t)}{dt} = (1 - \varphi)\gamma E - (\lambda + \mu)U \quad (5)$$

The Infected population (I) consists of individuals with Lassa fever. It fluctuates over time due to transmission, mortality, and other factors. The population size is influenced by infection rates and mortality.

$$\frac{dI(t)}{dt} = \gamma_2 \gamma E - (\omega + \mu + \sigma)I \quad (6)$$

The Recovered (R) compartment includes those who recovered, died, or were removed for other reasons. Flow depends on recovery, mortality, and elimination rates..

$$\frac{dR(t)}{dt} = \sigma I + \psi V_2 - \mu R + \lambda U \quad (7)$$

The SV1V2EUIR model simulates Lassa fever dynamics, assessing the impact of vaccination on disease spread. It is based on a system of differential equations derived from formulations (1) through (7).

$$\left. \begin{aligned} \frac{dS(t)}{dt} &= \pi + \varepsilon V_1 - \beta SI - (\rho + \mu)S \\ \frac{dV_1(t)}{dt} &= \rho S - (\varepsilon + \kappa + \mu)V_1 \\ \frac{dV_2(t)}{dt} &= \kappa V_1 - (\psi + \mu)V_2 \\ \frac{dE(t)}{dt} &= \beta SI - (\gamma_1 + \mu)E \\ \frac{dU(t)}{dt} &= (1 - \varphi)\gamma E - (\lambda + \mu)U \\ \frac{dI(t)}{dt} &= \varphi\gamma E - (\omega + \mu + \sigma)I \\ \frac{dR(t)}{dt} &= \sigma I + \psi V_2 - \mu R + \lambda U \end{aligned} \right\} \quad (8)$$

#### Model Assumptions:

The model assumptions for a double-dose Lassa vaccination strategy:

To activate the immune system, the initial dosage of the vaccine (V1) provides short-term immunity, but it might not offer complete protection, potentially increasing vulnerability. The immune response is strengthened by the second dose (V2), which provides longer-lasting immunity and indicates healing and well-being. While some vaccinations may require recurring booster shots to maintain protection, after V2, the immune system develops a strong memory response, reducing the likelihood of contracting the illness again. Strong immune memory is developed following the second dose (V2), resulting in sustained immunity and decreased susceptibility, even after a significant decrease in V2's effect. These assumptions pertain to the role of boosters in vaccination regimens and the activation of biological principles. However, factors such as the illness, the vaccine, and personal variables can all influence the duration of immunity and susceptibility.

Table 1 above variables, parameter and definition of each compartment in model Eq. (8).

$$u_3 = \frac{dV_2(t)}{dt} = \kappa V_1 - (\psi + \mu)V_2, \tag{9}$$

**(Theorem 1) Existence and Uniqueness of solution**

Let:

$$u_4 = \frac{dE(t)}{dt} = \beta SI - (\gamma + \mu)E,$$

$$u_1 = \frac{dS(t)}{dt} = \pi + \varepsilon V_1 - \beta SI - (\rho + \mu)S,$$

$$u_5 = \frac{dU(t)}{dt} = (1 - \varphi)\gamma E - (\lambda + \mu)U,$$

$$u_2 = \frac{dV_1(t)}{dt} = \rho S - (\varepsilon + \kappa + \mu)V,$$

$$u_6 = \frac{dI(t)}{dt} = \varphi\gamma E - (\omega + \mu + \sigma)I$$

$$u_7 = \frac{dR(t)}{dt} = \sigma I + \psi V_2 - \mu R + \lambda U$$

$$\mathfrak{R} = \left\{ (S(t), V_1(t), V_2(t), E(t), U(t), I(t), R(t)) : |S - S_0| \leq a, |V_1 - V_{10}| \leq b, |V_2 - V_{20}| \leq c, \right. \\ \left. |E - E_0| \leq d, |U - U_0| \leq e, |I - I_0| \leq f, |R - R_0| \leq g \right\}$$

The model's solution is distinct, using a partial derivative to produce the following;

$$\left| \frac{\partial u_1}{\partial S} \right| = |\beta - (\mu + \rho)|, \left| \frac{\partial u_1}{\partial V_1} \right| = |\varepsilon|, \left| \frac{\partial u_1}{\partial V_2} \right| = 0, \left| \frac{\partial u_1}{\partial E} \right| = 0, \left| \frac{\partial u_1}{\partial U} \right| = 0, \left| \frac{\partial u_1}{\partial I} \right| = |\beta|, \left| \frac{\partial u_1}{\partial R} \right| = 0$$

$$\left| \frac{\partial u_2}{\partial S} \right| = \rho, \left| \frac{\partial u_2}{\partial V_1} \right| = |-(\varepsilon + \kappa + \mu)|, \left| \frac{\partial u_2}{\partial V_2} \right| = 0, \left| \frac{\partial u_2}{\partial E} \right| = 0, \left| \frac{\partial u_2}{\partial U} \right| = 0, \left| \frac{\partial u_2}{\partial I} \right| = 0, \left| \frac{\partial u_2}{\partial R} \right| = 0,$$

$$\left| \frac{\partial u_3}{\partial S} \right| = 0, \left| \frac{\partial u_3}{\partial V_1} \right| = \kappa, \left| \frac{\partial u_3}{\partial V_2} \right| = |-(\psi + \mu)|, \left| \frac{\partial u_3}{\partial E} \right| = 0, \left| \frac{\partial u_3}{\partial U} \right| = 0, \left| \frac{\partial u_3}{\partial I} \right| = 0, \left| \frac{\partial u_3}{\partial R} \right| = 0$$

$$\left| \frac{\partial u_4}{\partial S} \right| = 0, \left| \frac{\partial u_4}{\partial V_1} \right| = 0, \left| \frac{\partial u_4}{\partial V_2} \right| = 0, \left| \frac{\partial u_4}{\partial E} \right| = |-(\gamma + \mu)|, \left| \frac{\partial u_4}{\partial U} \right| = 0, \left| \frac{\partial u_4}{\partial I} \right| = 0, \left| \frac{\partial u_4}{\partial R} \right| = 0$$

$$\left| \frac{\partial u_5}{\partial S} \right| = 0, \left| \frac{\partial u_5}{\partial V_1} \right| = 0, \left| \frac{\partial u_5}{\partial V_2} \right| = 0, \left| \frac{\partial u_5}{\partial E} \right| = (1 - \varphi)\gamma, \left| \frac{\partial u_5}{\partial U} \right| = |-(\lambda + \mu)|, \left| \frac{\partial u_5}{\partial I} \right| = 0, \left| \frac{\partial u_5}{\partial R} \right| = 0$$

$$\left| \frac{\partial u_6}{\partial S} \right| = 0, \left| \frac{\partial u_6}{\partial V_1} \right| = 0, \left| \frac{\partial u_6}{\partial V_2} \right| = 0, \left| \frac{\partial u_6}{\partial E} \right| = \varphi\gamma, \left| \frac{\partial u_6}{\partial U} \right| = 0, \left| \frac{\partial u_6}{\partial I} \right| = |-(\omega + \mu + \sigma)|, \left| \frac{\partial u_6}{\partial R} \right| = 0$$

$$\left| \frac{\partial u_7}{\partial S} \right| = 0, \left| \frac{\partial u_7}{\partial V_1} \right| = 0, \left| \frac{\partial u_7}{\partial V_2} \right| = \psi, \left| \frac{\partial u_7}{\partial E} \right| = 0, \left| \frac{\partial u_7}{\partial U} \right| = \lambda, \left| \frac{\partial u_7}{\partial I} \right| = \sigma, \left| \frac{\partial u_7}{\partial R} \right| = \mu$$

**Table 1** Variables and parameters description

S(t)	Susceptible at t
$V_1(t)$	Dose1at t
$V_2(t)$	Dose2 at t
$E(t)$	Exposed at t
$U(t)$	Infected Undetected at t
$I(t)$	Infected at t
$R(t)$	Recovered at t
$\pi$	Birth rate
$\mu$	Nature death rate
$\beta$	Transmission rate
$\rho$	first vaccine rate
$\kappa$	second vaccination rate
$\epsilon$	Waning first Vaccine rate
$\psi$	Immured offer second dose fully recovered rate
$\gamma$	Incubation rate exposed individual progress to infected individual
$\varphi$	Rate of infection progression from undiscovered to infected person
$\sigma$	Recovery rate of infected individual
$\omega$	Death induced due to disease
$\lambda$	Rate of recovery for an infected but unidentified person

Theorem 1 highlights the partial derivative’s biological viability and epidemiological significance by establishing boundaries and continuity for it in order to guarantee that the model is well-posed with a unique solution.

**Basic reproduction number**

Basic Reproduction Number ( $R_0$ ) which represents the average number of new cases brought on by one sick person, indicates how contagious a disease is. The sickness spreads if  $R_0 > 1$  and diminishes if  $R_0 < 1$ .  $R_0$  directs control methods like vaccination to lower transmission and aids in setting the herd immunity threshold.

$$R_0 = \frac{(\epsilon + \kappa + \mu)\pi\beta\gamma\varphi}{(\epsilon\mu + \kappa\mu + \kappa\rho + \mu^2 + \mu\rho)(\omega\mu + \sigma\varphi + \mu\varphi + \mu^2 + \mu\sigma + \omega\varphi)} \tag{10}$$

**Table 3** Impact of booster dose vaccine on  $R_0$

S/N	$\rho$	$\epsilon$	$\kappa$	$R_0$
1	0	0	0	0.00008
2	0.25	0.25	0.25	0.00004
3	0.45	0.45	0.45	0.00003
4	0.65	0.65	0.65	0.00002
5	0.85	0.85	0.85	0.000019
6	1.0	1.0	1.0	0.000013

**Analysis of Basic reproduction number**

If  $R_0 < 1$ , the disease is likely to fade out, while if  $R_0 > 1$ , it can lead to an epidemic and how vaccination control, the impact on  $R_0$  will be analyzed using estimated parameters from vaccination.  $R_0 = \frac{0.00001094017094(\epsilon + \kappa + 0.125)}{\kappa\rho + 0.125\kappa + 0.125\rho + 0.125\epsilon + 0.015625}$

Evaluates the effects of waning immunity, initial vaccination, and booster doses on reproduction number. The initial analysis focuses on waning and first vaccination variations, as shown in Table 2, while Table 3 presents a comprehensive assessment of their combined effects.

Lassa vaccine effectiveness without full coverage is demonstrated by Table 2A, which shows that waning vaccination lowers  $R_0$  below 1. Table 2B shows that first-dose vaccination effectively reduces  $R_0$ , promoting disease-free stability. Table 2C shows that combining first-dose and waning strategies accelerates  $R_0$  reduction. Table 3 highlights the combined effect, lowering  $R_0$  from 2 to below 1, suggesting the disease may die out.

**Sensitivity analysis of  $\mathfrak{R}_0$**

This analysis is performed using  $S_y^{\mathfrak{R}_0} = \frac{\partial \mathfrak{R}_0}{\partial y} \cdot \frac{y}{\mathfrak{R}_0}$ .

Table 4 presents the sensitivity analysis of parameters influencing disease spread. Recruitment rate and transmission coefficient are positively affect  $R_0$ , while recovery rate reduces it. Vaccination rates (first and second doses)

**Table 2** Solo and combined impact of first vaccination and waning first vaccination on  $R_0$

A					B				C			
S/N	$\rho$	$\epsilon$	$\kappa$	$R_0$	$\rho$	$\epsilon$	$\kappa$	$R_0$	$\rho$	$\epsilon$	$\kappa$	$R_0$
1	0	0	0	0.00009	0.9	0	0	0.00001	0.9	0.02	0	0.00005
2	0.25	0	0	0.00003	0.9	0.25	0	0.00003	0.9	0.02	0.25	0.00001
3	0.45	0	0	0.00002	0.9	0.45	0	0.00003	0.9	0.02	0.45	0.00001
4	0.65	0	0	0.00001	0.9	0.65	0	0.00004	0.9	0.02	0.65	0.00001
5	0.85	0	0	0.00001	0.9	0.85	0	0.00004	0.9	0.02	0.85	0.00001
6	1.0	0	0	0.000001	0.9	1.0	0	0.00005	0.9	0.02	1,0	0.00002

negatively impact  $R_0$ , highlighting the role of increased vaccination efforts. However, waning immunity from the first dose raises  $R_0$ , emphasizing the need for booster doses and awareness programs.

Booster uptake further reduces  $R_0$ , underlining its importance. Factors like contact rate and the progression of exposed individuals to undetected infection also increase  $R_0$ , stressing the need for mitigation efforts. Enhancing vaccination, reducing contact rates, and implementing screening and treatment are crucial for controlling Lassa disease. Figures 1 and 2 show the sensitivity indices on  $R_0$  respectively.

**Stability analysis**

Disease dynamics are evaluated using stability analysis of the Disease-Free Equilibrium (DFE) and Endemic Equilibrium (EEP) in Lassa fever models. The DFE is stable if the basic reproduction number  $R_0 < 1$ , indicating the possibility of eliminating the disease with appropriate health interventions. The EEP is stable when  $R_0 > 1$ , suggesting that the disease will persist and need to be targeted with vaccination to prevent and control Lassa fever outbreaks.

**Disease free equilibrium**

$E = I = Q = 0$ . Equating Eq. (8) to zero yields:

$$E_0 = (S^*, V1^*, V2^*, E^*, U^*, I^*, R^*) = \left( \frac{\pi(\varepsilon + \kappa + \mu)}{\varepsilon\mu + \mu^2 + \kappa\rho + \mu\rho}, \frac{\pi\rho}{\varepsilon\mu + \mu^2 + \kappa\rho + \mu\rho}, \frac{\pi\kappa\rho}{\varepsilon\mu\psi + \varepsilon\mu^2 + \kappa\mu^2 + \mu\kappa\psi + \kappa\mu\rho + \kappa\psi\rho + \mu^3 + \mu^2\psi + \mu^2\rho + \mu\psi\rho}, 0, 0, 0, 0 \right) \tag{11}$$

**Table 4** Sensitivity index of each parameter on  $R_0$

Parameters	Sensitivity indices
$\rho$	- 0.8559298048
$\beta$	1
$\varepsilon$	0.3417607759
$\gamma$	0.3846153844
$\mu$	- 1.232714941
$\pi$	1
$\kappa$	- 0.001187790446
$\omega$	- 0.08888888892
$\sigma$	0.6444444433

**Endemic equilibrium**

$E_1 = (S^{**}, V1^{**}, V2^{**}, E^{**}, U^{**}, I^{**}, R^{**})$  is obtained as follows.

$$S^{**} = \frac{\mu\gamma + \gamma\omega + \gamma\sigma + \mu^2 + \mu\omega + \mu\sigma}{\gamma\phi\beta} \tag{12}$$

$$V1^{**} = \frac{\rho(\gamma\mu + \gamma\omega + \gamma\sigma + \mu^2 + \mu\omega + \mu\sigma)}{(\varepsilon + \kappa + \mu)\gamma\beta\phi} \tag{13}$$

$$V2^{**} = \frac{\rho\kappa(\gamma\mu + \gamma\omega + \gamma\sigma + \mu^2 + \mu\omega + \mu\sigma)}{(\varepsilon\mu + \varepsilon\psi + \gamma\sigma + \kappa\mu + \kappa\psi + \mu^2 + \mu\psi)\gamma\beta\phi} \tag{14}$$

$$E^{**} = \frac{1}{(\varepsilon\gamma + \varepsilon\mu + \gamma\sigma + \kappa\gamma + \gamma\mu + \mu^2 + \mu\kappa)\gamma\phi} (-\mu^2\rho\sigma - \mu^2\rho\omega - \mu^2\varepsilon\sigma - \mu^2\varepsilon\omega - \mu^2\rho\gamma - \mu^2\gamma\varepsilon - \mu^2\gamma\omega - \mu^2\gamma\sigma - \mu^2\kappa\gamma - \mu^2\kappa\omega - \mu^2\kappa\sigma - \mu^3\kappa - \mu^3\omega - \mu^3\sigma - \mu^3\gamma - \mu^2\rho\kappa - \mu\gamma\omega\kappa - \mu\gamma\sigma\kappa - \mu\gamma\rho\kappa - \gamma\omega\rho\kappa - \gamma\sigma\rho\kappa - \gamma\omega\rho\mu - \gamma\mu\rho\sigma - \gamma\omega\varepsilon\mu - \gamma\varepsilon\sigma\mu - \mu\omega\rho\kappa - \mu\sigma\rho\kappa + \pi\phi\varepsilon\beta\gamma + \pi\phi\kappa\beta\gamma + \pi\phi\mu\beta\gamma - \mu^4 - \mu^3\rho - \mu^3\varepsilon) \tag{15}$$

$$U^{**} = \frac{1}{\phi(\lambda + \mu)(\varepsilon\gamma + \varepsilon\mu + \gamma\sigma + \kappa\gamma + \gamma\mu + \mu^2 + \mu\kappa)\beta} ((\phi - 1)(-\mu^2\rho\sigma - \mu^2\rho\omega - \mu^2\varepsilon\sigma - \mu^2\varepsilon\omega - \mu^2\rho\gamma - \mu^2\gamma\varepsilon - \mu^2\gamma\omega - \mu^2\kappa\gamma - \mu^2\kappa\omega - \mu^2\kappa\sigma - \mu^3\kappa - \mu^3\omega - \mu^3\sigma - \mu^3\gamma - \mu^2\rho\kappa - \mu\gamma\omega\kappa - \mu\gamma\sigma\kappa - \mu\gamma\rho\kappa - \gamma\omega\rho\kappa - \gamma\sigma\rho\kappa - \gamma\omega\rho\mu - \gamma\mu\rho\sigma - \gamma\omega\varepsilon\mu - \gamma\varepsilon\sigma\mu - \mu\omega\rho\kappa - \mu\sigma\rho\kappa + \pi\phi\varepsilon\beta\gamma + \pi\phi\kappa\beta\gamma + \pi\phi\mu\beta\gamma - \mu^4 - \mu^3\rho - \mu^3\varepsilon)) \tag{16}$$

$$I^{**} = \frac{\begin{pmatrix} -\mu^2\rho\sigma - \mu^2\rho\omega - \mu^2\varepsilon\sigma - \mu^2\varepsilon\omega - \mu^2\rho\gamma - \mu^2\gamma\varepsilon - \mu^2\gamma\omega - \mu^2\gamma\sigma - \mu^2\kappa\gamma - \mu^2\kappa\omega - \mu^2\kappa\sigma \\ -\mu^3\kappa - \mu^3\omega - \mu^3\sigma - \mu^3\gamma - \mu^2\rho\kappa - \mu\gamma\omega\kappa - \mu\gamma\sigma\kappa - \mu\gamma\rho\kappa - \gamma\omega\rho\kappa - \gamma\sigma\rho\kappa - \gamma\omega\rho\mu - \gamma\mu\rho\sigma \\ -\gamma\omega\varepsilon\mu - \gamma\varepsilon\sigma\mu - \mu\omega\rho\kappa - \mu\sigma\rho\kappa + \pi\varphi\varepsilon\beta\gamma + \pi\varphi\kappa\beta\gamma + \pi\varphi\mu\beta\gamma - \mu^4 - \mu^3\rho - \mu^3\varepsilon \end{pmatrix}}{\beta(\varepsilon\gamma\mu + \varepsilon\mu\omega + \varepsilon\gamma\sigma + \omega\kappa\gamma + \gamma\mu\omega + \gamma\mu^2 + \gamma\mu\kappa + \gamma\mu\sigma + \kappa\mu^2 + \omega\mu\kappa + \sigma\mu\kappa + \mu^3 + \mu^2\omega + \mu^2\sigma)}$$

**The new fractional Caputo derivative Model designed**

$$\left. \begin{aligned} {}^cD^{\alpha_1}S(t) &= \pi + \varepsilon V_1 - \beta SI - (\rho + \mu)S \\ {}^cD^{\alpha_1}V_1(t) &= \rho S - (\varepsilon + \kappa + \mu)V_1 \\ {}^cD^{\alpha_1}V_2(t) &= \kappa V_1 - (\psi + \mu)V_2 \\ {}^cD^{\alpha_1}E(t) &= \beta SI - (\gamma + \mu)E \\ {}^cD^{\alpha_1}U(t) &= (1 - \varphi)\gamma E - (\lambda + \mu)U \\ {}^cD^{\alpha_1}I(t) &= \varphi\gamma E - (\omega + \mu + \sigma)I \\ {}^cD^{\alpha_1}R(t) &= \sigma I + \psi V_2 - \mu R + \lambda U \end{aligned} \right\} \quad (18)$$

With initial condition  $S_0 = n_1, V_{10} = n_2, V_{20} = n_3, E_0 = n_4, U_0 = n_5, I_0 = n_6, R_0 = n_7$ .  
 ${}^cD^{\alpha} \leq \alpha \leq 1$  Caputo's derivative of fractional order and  $\alpha$  fractional time derivative.

**The Laplace Adomian decomposition method**

Applying Laplace transform to both side of model (18)

$$\left. \begin{aligned} L\{{}^cD^{\alpha_1}S(t)\} &= L\{\pi + \varepsilon V_1 - \beta SI - (\rho + \mu)S\} \\ L\{{}^cD^{\alpha_2}V_1(t)\} &= L\{\rho S - (\varepsilon + \kappa + \mu)V_1\} \\ L\{{}^cD^{\alpha_3}V_2(t)\} &= L\{\kappa V_1 - (\psi + \mu)V_2\} \\ L\{{}^cD^{\alpha_4}E(t)\} &= L\{\beta SI - (\gamma + \mu)E\} \\ L\{{}^cD^{\alpha_5}U(t)\} &= L\{(1 - \varphi)\gamma E - (\lambda + \mu)U\} \\ L\{{}^cD^{\alpha_6}I(t)\} &= L\{\varphi\gamma E - (\omega + \mu + \sigma)I\} \\ L\{{}^cD^{\alpha_7}R(t)\} &= L\{\sigma I + \psi V_2 - \mu R + \lambda U\} \end{aligned} \right\} \quad (19)$$

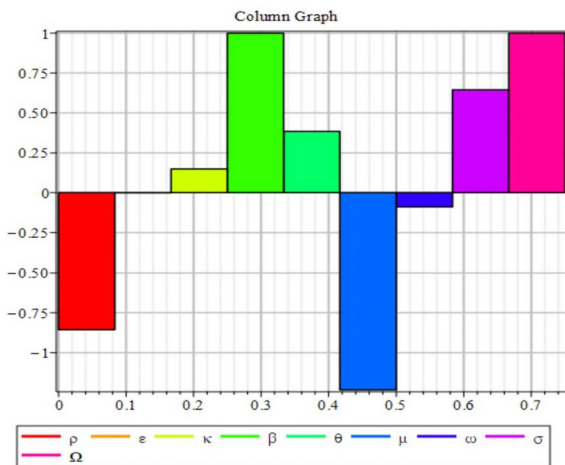


**Fig. 1** Sensitivity chart of parameter on  $S_0$

**Solving (19)**

$$\left. \begin{aligned} S(t) &= S^{-1}S(0) + \frac{1}{S^{\alpha_1}}L\{\pi + \varepsilon V_1 - \beta SI - (\rho + \mu)S\} \\ V_1(t) &= S^{-1}V_1(0) + \frac{1}{S^{\alpha_2}}L\{\rho S - (\varepsilon + \kappa + \mu)V_1\} \\ V_2(t) &= S^{-1}V_2(0) + \frac{1}{S^{\alpha_3}}L\{\kappa V_1 - (\psi + \mu)V_2\} \\ E(t) &= S^{-1}E(0) + \frac{1}{S^{\alpha_4}}L\{\beta SI - (\gamma + \mu)E\} \\ U(t) &= S^{-1}U(0) + \frac{1}{S^{\alpha_5}}L\{(1 - \varphi)\gamma E - (\lambda + \mu)U\} \\ I(t) &= S^{-1}I(0) + \frac{1}{S^{\alpha_6}}L\{\varphi\gamma E - (\omega + \mu + \sigma)I\} \\ R(t) &= S^{-1}R(0) + \frac{1}{S^{\alpha_7}}L\{\sigma I + \psi V_2 - \mu R + \lambda U\} \end{aligned} \right\} \quad (20)$$

$S(t), V_1(t), V_2(t), E(t), U(t), I(t), R(t)$  infinite series

$$\left. \begin{aligned} S(t) &= \sum_{n=0}^{\infty} S_n, V_1(t) = \sum_{n=0}^{\infty} V_{1n}, \\ V_2(t) &= \sum_{n=0}^{\infty} V_{2n}, E(t) = \sum_{n=0}^{\infty} E_n, U(t) = \sum_{n=0}^{\infty} U_n, \\ I(t) &= \sum_{n=0}^{\infty} I_n, R(t) = \sum_{n=0}^{\infty} R_n, \end{aligned} \right\} \quad (21)$$

**Using initial condition**

$$\left. \begin{aligned} S(t) &= S^{-1}S(0) + \frac{1}{S^{\alpha_1}}L\{\pi + \varepsilon V_1 - \beta SI - (\rho + \mu)S\} \\ V_1(t) &= S^{-1}V_1(0) + \frac{1}{S^{\alpha_2}}L\{\rho S - (\varepsilon + \kappa + \mu)V_1\} \\ V_2(t) &= S^{-1}V_2(0) + \frac{1}{S^{\alpha_3}}L\{\kappa V_1 - (\psi + \mu)V_2\} \\ E(t) &= S^{-1}E(0) + \frac{1}{S^{\alpha_4}}L\{\beta SI - (\gamma + \mu)E\} \\ U(t) &= S^{-1}U(0) + \frac{1}{S^{\alpha_5}}L\{(1 - \varphi)\gamma E - (\lambda + \mu)U\} \\ I(t) &= S^{-1}I(0) + \frac{1}{S^{\alpha_6}}L\{\varphi\gamma E - (\omega + \mu + \sigma)I\} \\ R(t) &= S^{-1}R(0) + \frac{1}{S^{\alpha_7}}L\{\sigma I + \psi V_2 - \mu R + \lambda U\} \end{aligned} \right\} \quad (22)$$

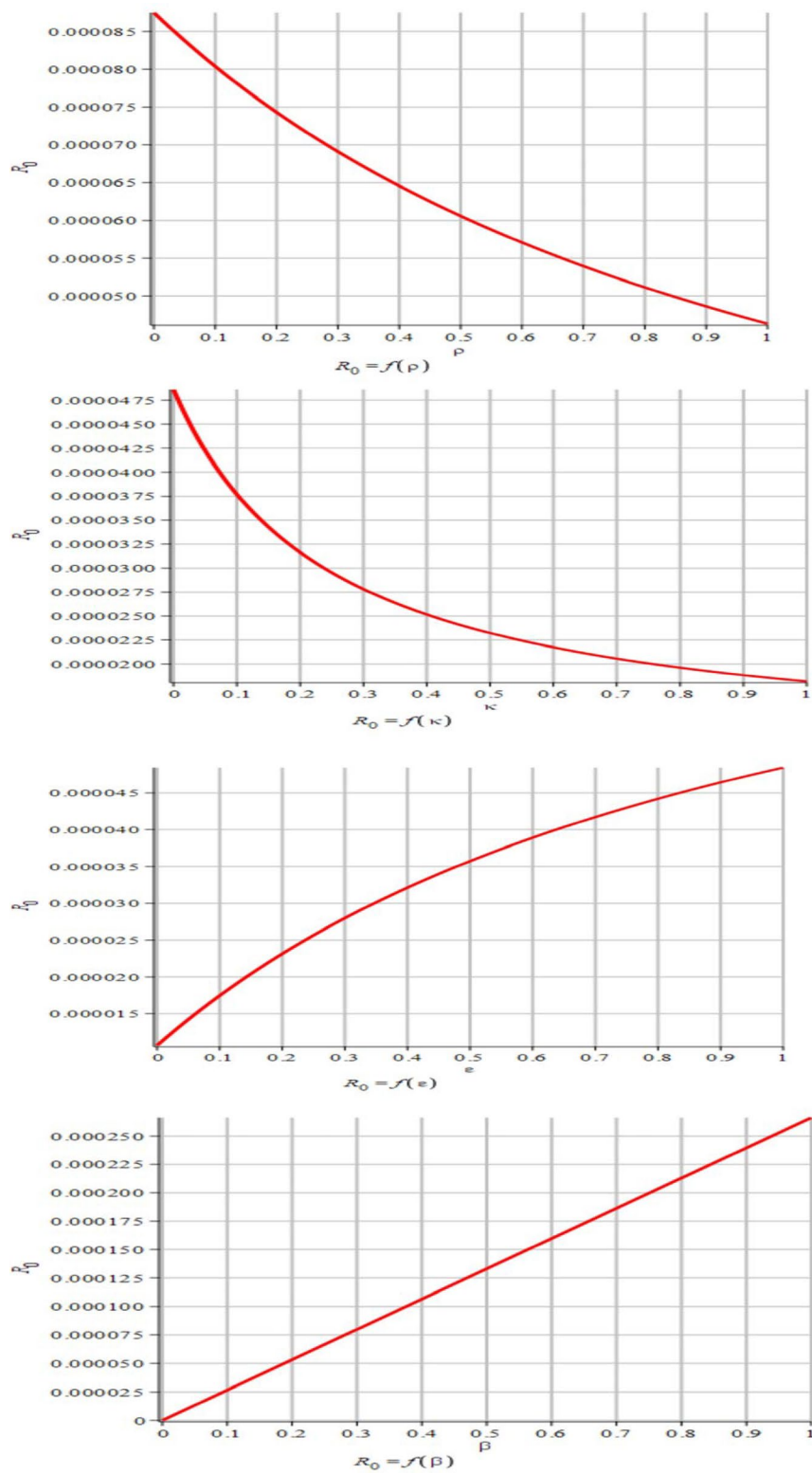


**Fig. 2** Simulated parameters on  $\mathfrak{R}_0$

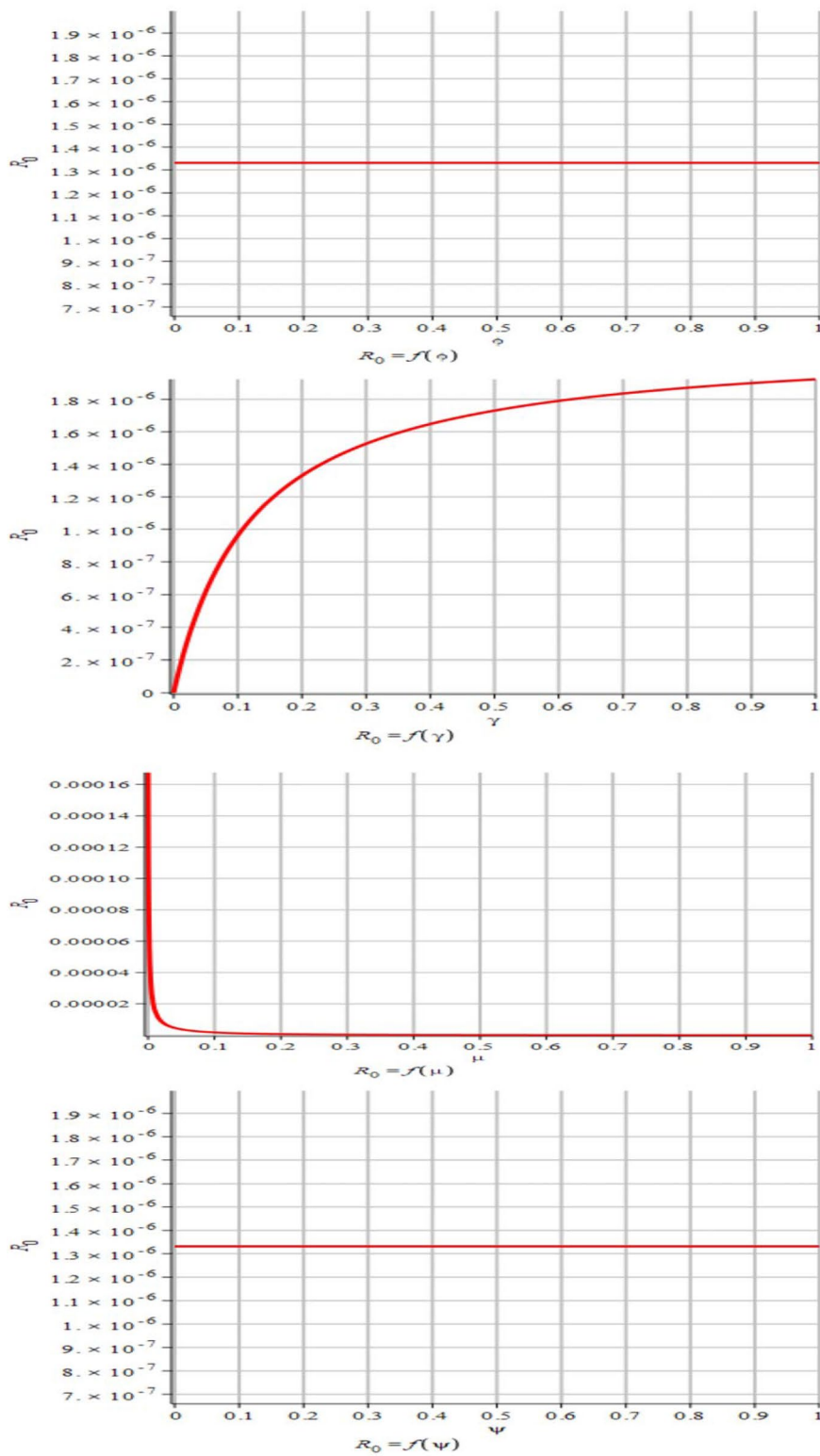


Fig. 2 continued

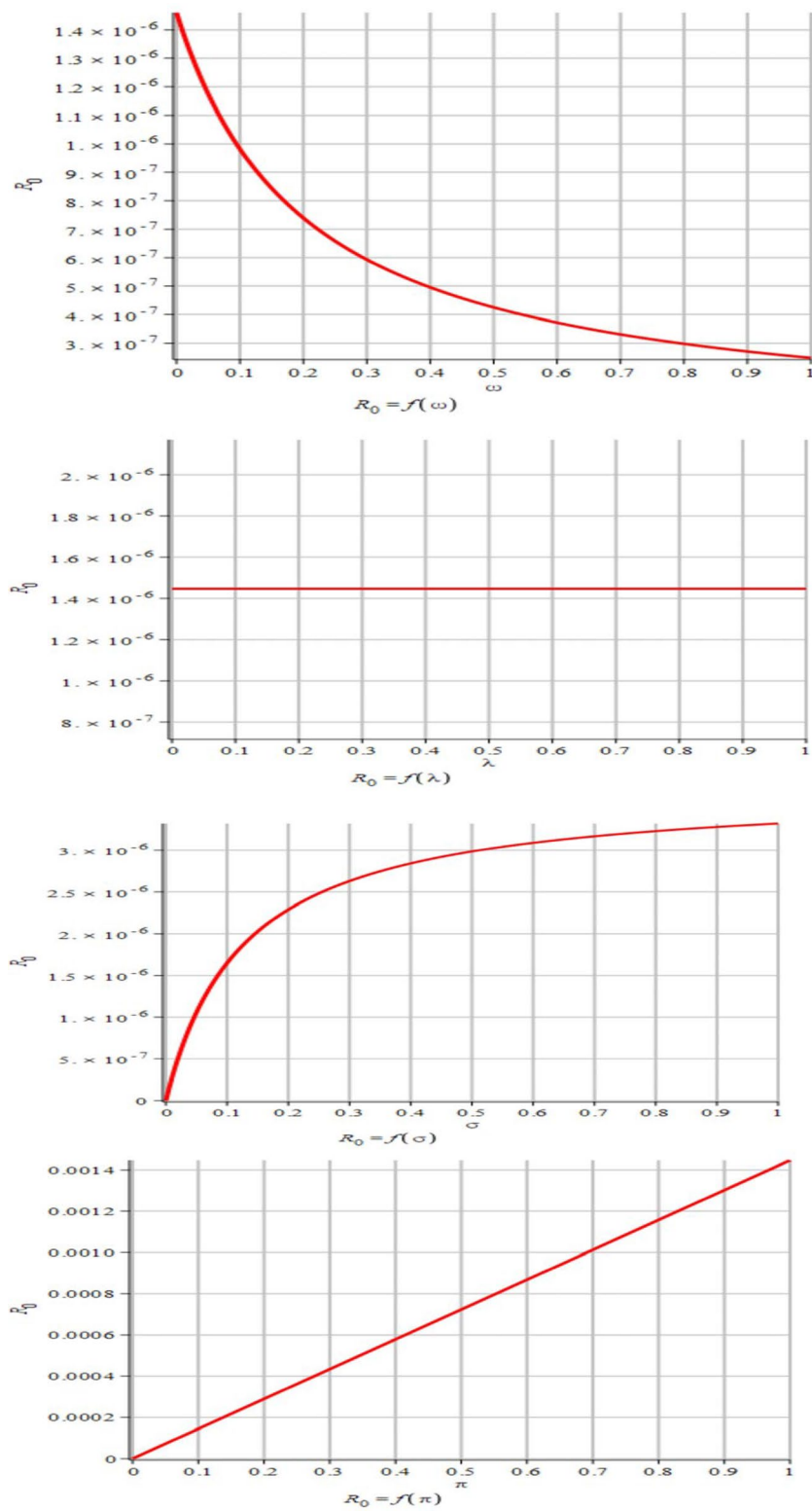


Fig. 2 continued

Laplace inverse gives General formula for the model

$$\left. \begin{aligned}
 \sum_{n=0}^{\infty} S_{n+1}(t) &= L^{-1} \left[ \frac{1}{S^{\alpha_1}} L\{\pi + \varepsilon V_1 - \beta SI - (\rho + \mu)S\} \right] \\
 \sum_{n=0}^{\infty} V_{1n+1}(t) &= L^{-1} \left[ \frac{1}{S^{\alpha_2}} L\{\rho S - (\varepsilon + \kappa + \mu)V_1\} \right] \\
 \sum_{n=0}^{\infty} V_{2n+1}(t) &= L^{-1} \left[ \frac{1}{S^{\alpha_3}} L\{\kappa V_1 - (\psi + \mu)V_2\} \right] \\
 \sum_{n=0}^{\infty} E_{n+1}(t) &= L^{-1} \left[ \frac{1}{S^{\alpha_4}} L\{\beta SI - (\gamma + \mu)E\} \right] \\
 \sum_{n=0}^{\infty} U_{n+1}(t) &= L^{-1} \left[ \frac{1}{S^{\alpha_5}} L\{(1 - \varphi)\gamma E - (\lambda + \mu)U\} \right] \\
 \sum_{n=0}^{\infty} I_{n+1}(t) &= L^{-1} \left[ \frac{1}{S^{\alpha_6}} L\{\varphi\gamma E - (\omega + \mu + \sigma)I\} \right] \\
 \sum_{n=0}^{\infty} R_{n+1}(t) &= L^{-1} \left[ \frac{1}{S^{\alpha_7}} L\{\sigma I + \psi V_2 - \mu R + \lambda U\} \right]
 \end{aligned} \right\} \tag{23}$$

$$\begin{aligned}
 S_1 &= (\pi + \varepsilon n_2 - \beta n_1 n_6 - (\rho + \mu)n_1) \frac{t^{\alpha_1}}{\Gamma(\alpha_1 + 1)} \\
 V_{11} &= (\rho n_1 - (\varepsilon + \kappa + \mu)n_2) \frac{t^{\alpha_2}}{\Gamma(\alpha_2 + 1)} \\
 V_{21} &= (\kappa n_2 - (\psi + \mu)n_3) \frac{t^{\alpha_3}}{\Gamma(\alpha_3 + 1)} \\
 E_1 &= (\beta n_1 n_6 - (\gamma + \mu)n_4) \frac{t^{\alpha_4}}{\Gamma(\alpha_4 + 1)} \\
 U_1 &= ((1 - \varphi)\gamma n_4 - (\lambda + \mu)n_5) \frac{t^{\alpha_5}}{\Gamma(\alpha_5 + 1)} \\
 I_1 &= (\varphi\gamma n_4 - (\omega + \mu + \sigma)n_6) \frac{t^{\alpha_6}}{\Gamma(\alpha_6 + 1)} \\
 R_1 &= (\sigma n_6 + \psi n_3 - \mu n_7 + \lambda n_5) \frac{t^{\alpha_7}}{\Gamma(\alpha_7 + 1)}
 \end{aligned}$$

Iterations

$$\begin{aligned}
 S_2 &= \pi + \varepsilon(\rho n_1 - (\varepsilon + \kappa + \mu)n_2) \frac{t^{\alpha_1 + \alpha_2}}{\Gamma(\alpha_1 + \alpha_2 + 1)} - \beta(n_1(\varphi\gamma n_4 - (\omega + \mu + \sigma)n_6) \frac{t^{\alpha_1 + \alpha_6}}{\Gamma(\alpha_1 + \alpha_6 + 1)} \\
 &\quad + n_6(\pi + \varepsilon n_2 - \beta n_1 n_6 - (\rho + \mu)n_1) \frac{t^{2\alpha_1}}{\Gamma(2\alpha_1 + 1)} - (\rho + \mu)(\pi + \varepsilon n_2 - \beta n_1 n_6 - (\rho + \mu)n_1) \frac{t^{2\alpha_1}}{\Gamma(2\alpha_1 + 1)} \\
 V_{12} &= \rho(\pi + \varepsilon n_2 - \beta n_1 n_6 - (\rho + \mu)n_1) \frac{t^{\alpha_1 + \alpha_2}}{\Gamma(\alpha_1 + \alpha_2 + 1)} - (\varepsilon_1 + k + \mu)(\rho n_1 - \varepsilon_1 n_2 - \kappa n_2 - \mu n_2) \frac{t^{2\alpha_2}}{\Gamma(2\alpha_2 + 1)} \\
 V_{22} &= \kappa(\rho n_1 - (\varepsilon + \kappa + \mu)n_2) \frac{t^{\alpha_2 + \alpha_3}}{\Gamma(\alpha_2 + \alpha_3 + 1)} - (\psi + \mu)(\kappa n_1 - \psi n_3 - \mu n_3) \frac{t^{2\alpha_3}}{\Gamma(2\alpha_3 + 1)} \\
 E_2 &= \beta \left( n_1(\varphi\gamma n_4 - (\omega + \mu + \sigma)n_6) \frac{t^{\alpha_1 + \alpha_6}}{\Gamma(\alpha_6 + \alpha_4 + 1)} + n_6(\pi + \varepsilon n_2 - \beta n_1 n_6 - (\rho + \mu)n_1) \frac{t^{\alpha_1 + \alpha_4}}{\Gamma(\alpha_1 + \alpha_4 + 1)} \right) \\
 &\quad - (\gamma + \mu)(\beta n_1 n_6 - (\gamma + \mu)n_4) \frac{t^{2\alpha_4}}{\Gamma(2\alpha_4 + 1)} \\
 U_2 &= (1 - \varphi)\gamma(\beta n_1 n_6 - (\gamma + \mu)n_4) \frac{t^{\alpha_5 + \alpha_4}}{\Gamma(\alpha_5 + \alpha_4 + 1)} - (\lambda + \mu)((1 - \varphi)\gamma n_4 - (\lambda + \mu)n_5) \frac{t^{2\alpha_5}}{\Gamma(2\alpha_5 + 1)} \\
 I_2 &= \varphi\gamma(\beta n_1 n_6 - (\gamma + \mu)n_4) \frac{t^{\alpha_4 + \alpha_6}}{\Gamma(\alpha_4 + \alpha_6 + 1)} - (\omega + \mu + \sigma)(\varphi\gamma n_4 - (\omega + \mu + \sigma)n_6) \frac{t^{\alpha_6}}{\Gamma(2\alpha_6 + 1)}
 \end{aligned}$$

$$R_2 = \sigma(\varphi\gamma n_4 - (\omega + \mu + \sigma)n_6) \frac{t^{\alpha_5 + \alpha_9}}{\Gamma(\alpha_6 + \alpha_7 + 1)} + \psi(\kappa n_2 - (\psi + \mu)n_3) \frac{t^{\alpha_7 + \alpha_9}}{\Gamma(\alpha_7 + \alpha_3 + 1)} - \mu(\sigma n_6 + \psi n_3 - \mu n_7 + \lambda n_5) \frac{t^{2\alpha_7}}{\Gamma(2\alpha_7 + 1)} + \psi(\kappa n_2 - (\psi + \mu)n_3) \frac{t^{\alpha_7 + \alpha_5}}{\Gamma(\alpha_7 + \alpha_5 + 1)}$$

**Numerical results**

Utilized initial values (S(0), V1(0), V2(0), E(0), U(0), I(0), R(0))=(200, 150, 110, 100, 90, 150, 180) and parameters values

$$\beta = 0.05 \quad \varphi = 0,5, \quad \gamma = 0.2, \quad \kappa = 0.001, \quad \mu = 0.125, \quad \psi = 0.1 \quad \omega = 0.02, \quad \sigma = 0.08, \quad \lambda = 0.3, \quad \pi = 0.001, \quad \rho = 0.9, \varepsilon = 0.0267$$

We obtain the following series solution:

$$S(t) = 200.001 - \frac{1700.9940t^\alpha}{\Gamma(\alpha + 1)} + \frac{14742.66829t^{2\alpha}}{\Gamma(2\alpha + 1)},$$

$$V_1(t) = 150 + \frac{157.0950t^\alpha}{\Gamma(\alpha + 1)} - \frac{1554.883006t^{2\alpha}}{\Gamma(2\alpha + 1)},$$

$$V_2(t) = 110 - \frac{24.600t^\alpha}{\Gamma(\alpha + 1)} + \frac{5.6920950t^{2\alpha}}{\Gamma(2\alpha + 1)}$$

$$E(t) = 100 + \frac{1467.500t^\alpha}{\Gamma(\alpha + 1)} + \frac{13471.89250t^{2\alpha}}{\Gamma(2\alpha + 1)}$$

$$U(t) = 90 - \frac{28.250t^\alpha}{\Gamma(\alpha + 1)} + \frac{158.756250t^{2\alpha}}{\Gamma(2\alpha + 1)}$$

$$I(t) = 150 - \frac{23.750t^\alpha}{\Gamma(\alpha + 1)} + \frac{152.093750t^{2\alpha}}{\Gamma(2\alpha + 1)}$$

$$R(t) = 180 + \frac{27.500t^\alpha}{\Gamma(\alpha + 1)} - \frac{16.272500t^{2\alpha}}{\Gamma(2\alpha + 1)}$$

**Discussions**

The model’s efficacy was validated by simulations, which showed that raising alpha improves immunization and recovery rates while slowing the spread of disease. The dynamics of vaccination, infection, and recovery are presented in Figs. 2, 3, 4, 5, 6, 7, offering a comprehensive

view of how these factors evolve over time. Figures 8, 9, 10, 11, 12, 13, 14, 15, 16, 17, 18, 19, on the other hand, underscore the critical importance of controlling

transmission to manage Lassa fever. Higher transmission rates are shown to result in significantly elevated peak exposures, which highlights the need for stringent measures to limit disease spread (Figs. 20, 21).

Moreover, population dynamics are profoundly influenced by adjustments to first- and second-dose vaccination rates. Notably, achieving higher second-dose coverage is pivotal in preventing the disease from becoming endemic and in enhancing recovery rates across the population. Vaccination continues to be one of the most effective and essential strategies for mitigating Lassa fever, underscoring its role in disease prevention and control.

**Conclusion**

The study employs a novel mathematical modeling approach using fractional Caputo derivatives to investigate the transmission of Lassa fever, the uniqueness of the model solution, and the reproduction number (R<sub>0</sub>). Numerical simulations reveal the impacts of both initial and subsequent vaccine doses, highlighting the critical role of higher vaccination rates in reducing infections and halting disease spread. The findings strongly advocate for mass vaccination campaigns to generate herd immunity, prevent outbreaks, and improve the precision of outbreak prediction models. In order to develop strong immunity in communities, the study emphasizes the significance of a comprehensive vaccination approach, especially the use of two-dose regimens. This study identifies a critical route to halting the development of Lassa fever and lessening its effects on public health by filling in vaccine gaps and encouraging mass immunization campaigns.

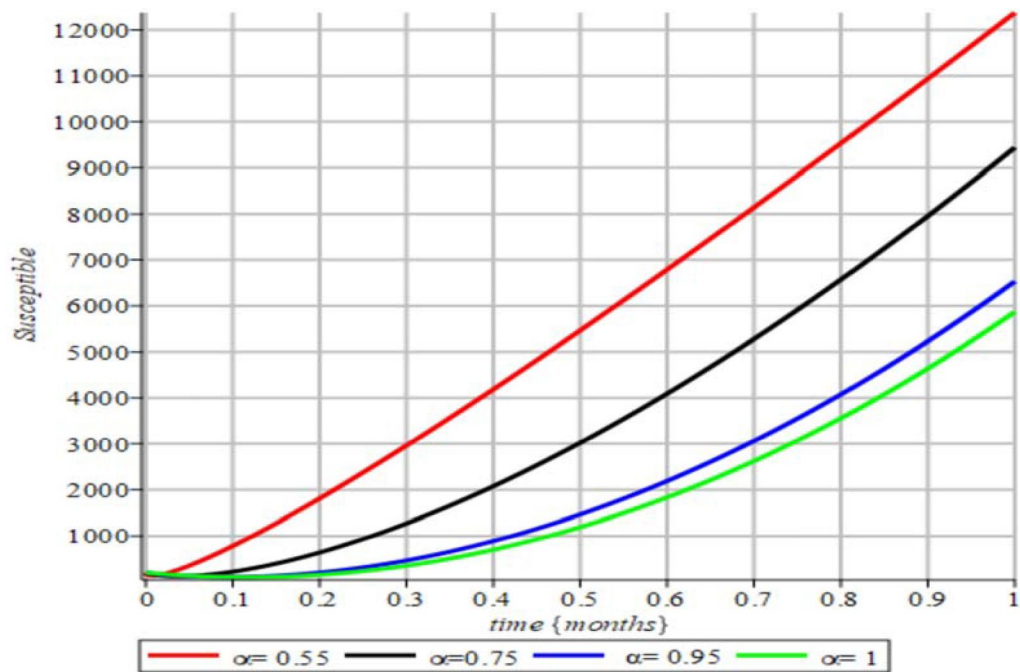


**Fig. 3** fractional order effect on susceptible

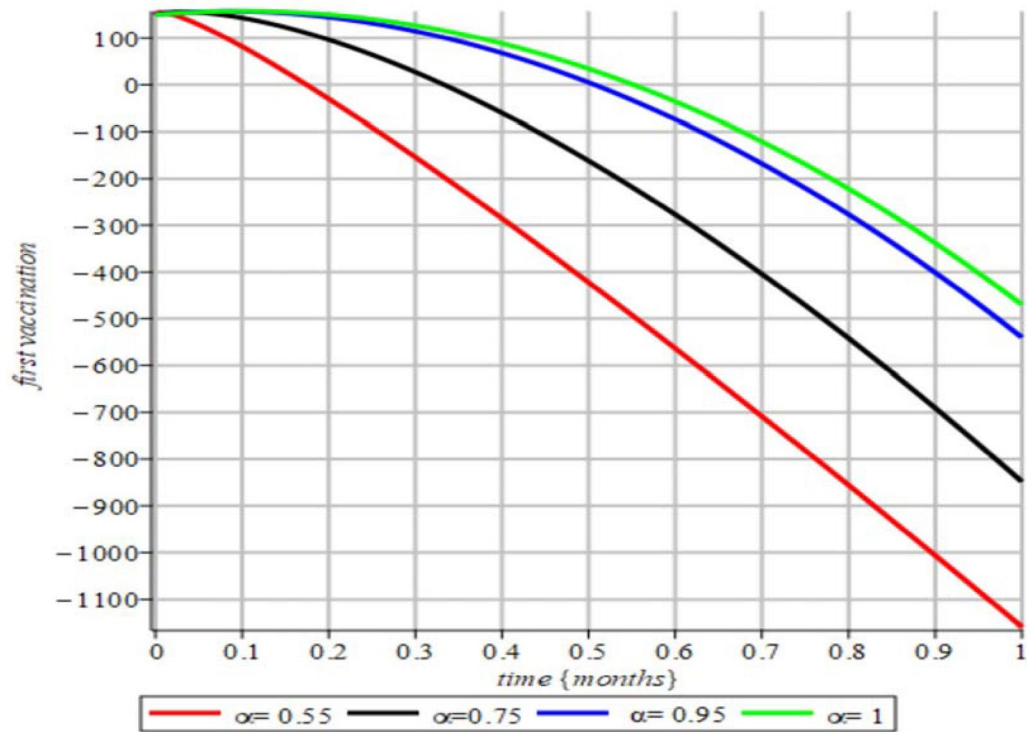


**Fig. 4** fractional order effect on first vaccination

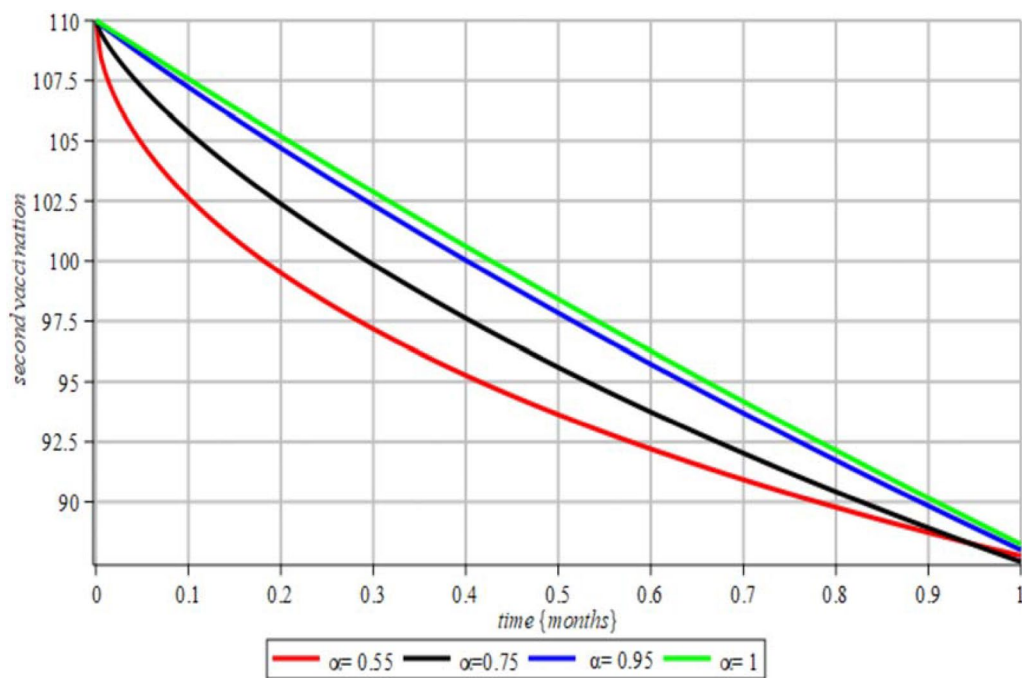


**Fig. 5** fractional order effect on second vaccination

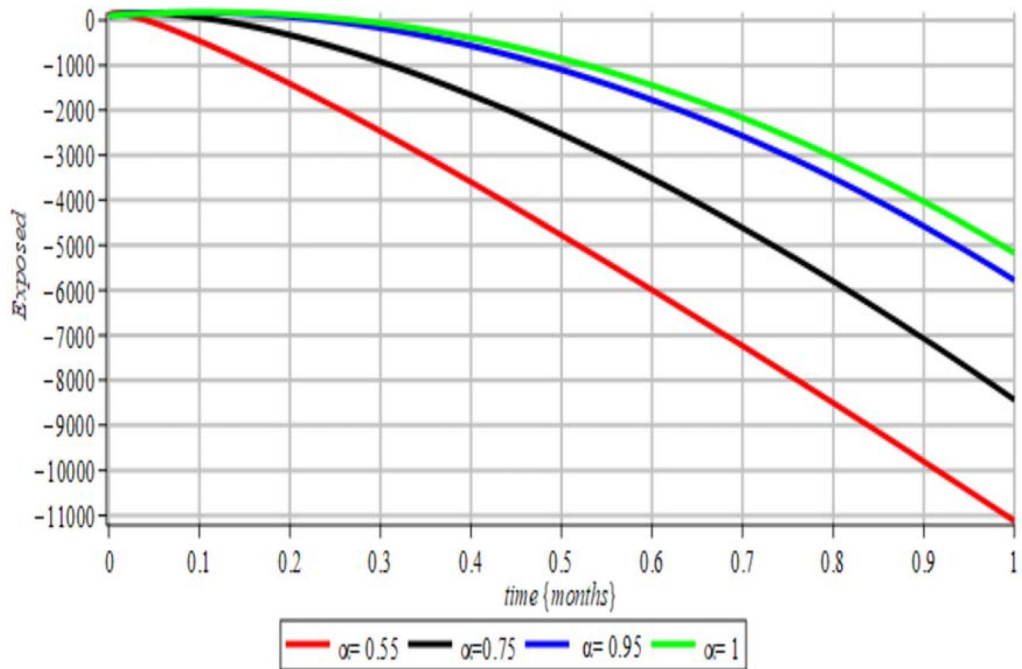


**Fig. 6** fractional order effect on Exposed

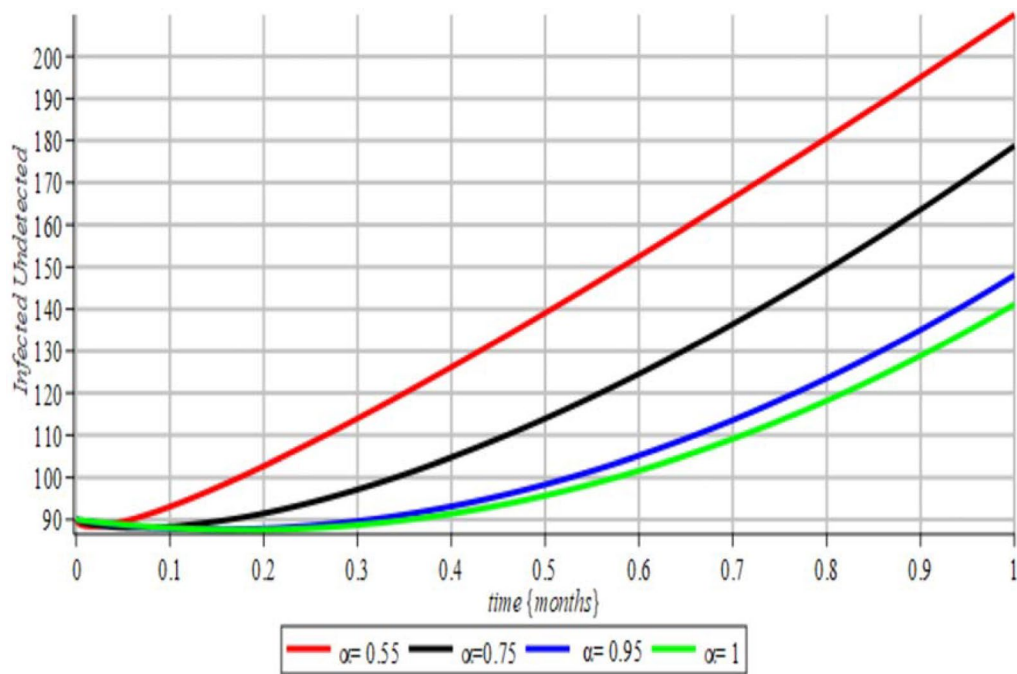


**Fig. 7** fractional order effect on infected undetected

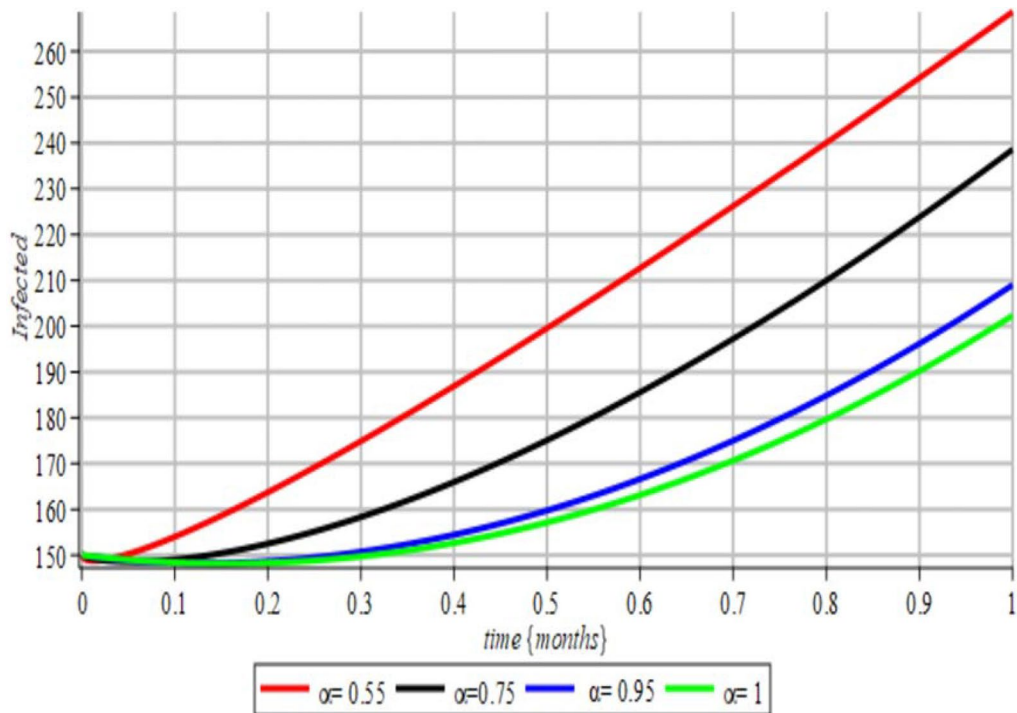


**Fig. 8** fractional order effect on infected

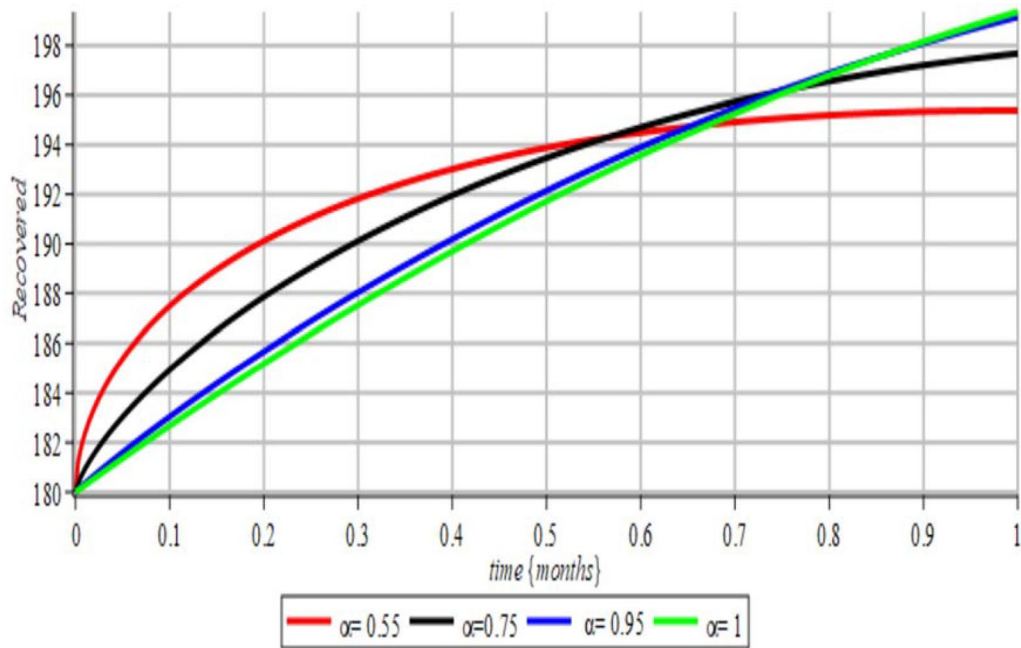


**Fig. 9** fractional order effect on Recovered

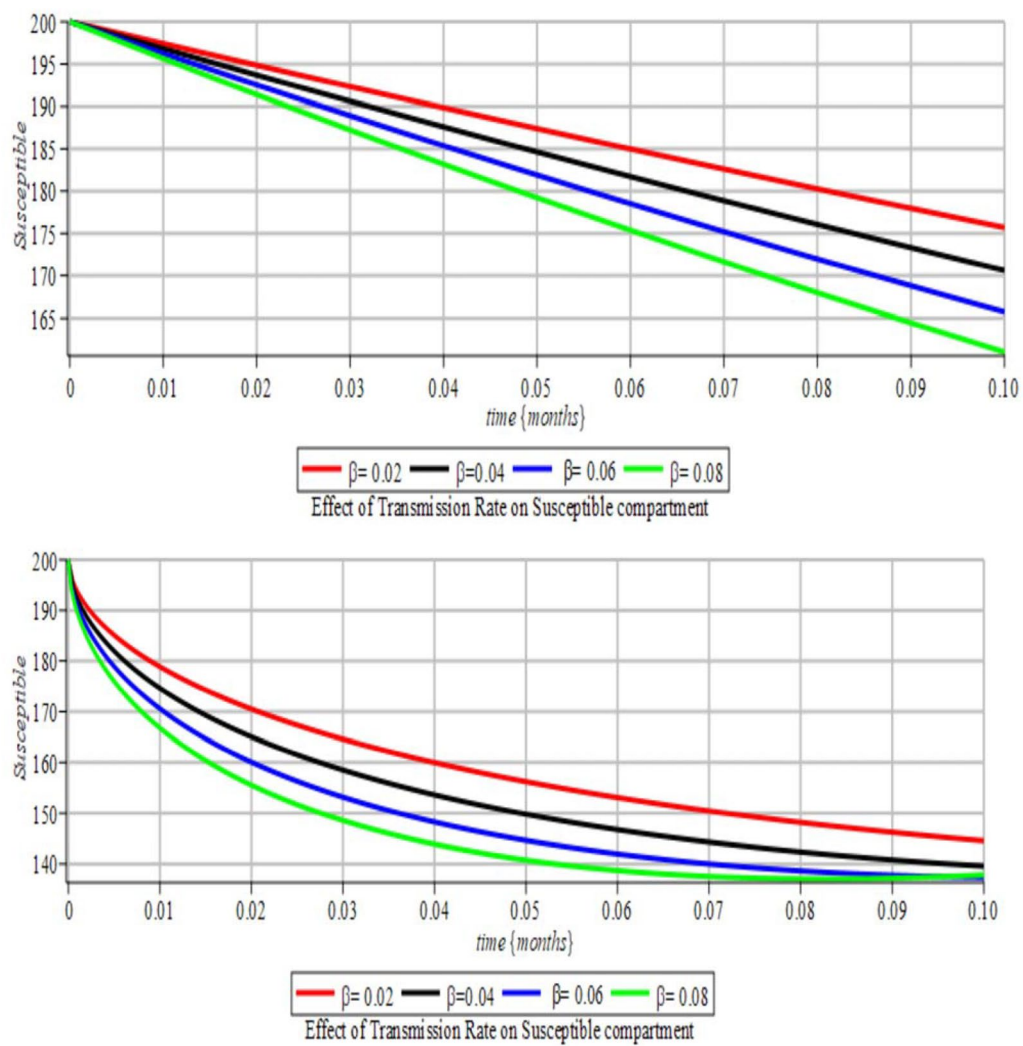


**Fig. 10** Effect of  $\beta$  on Classical and fractional

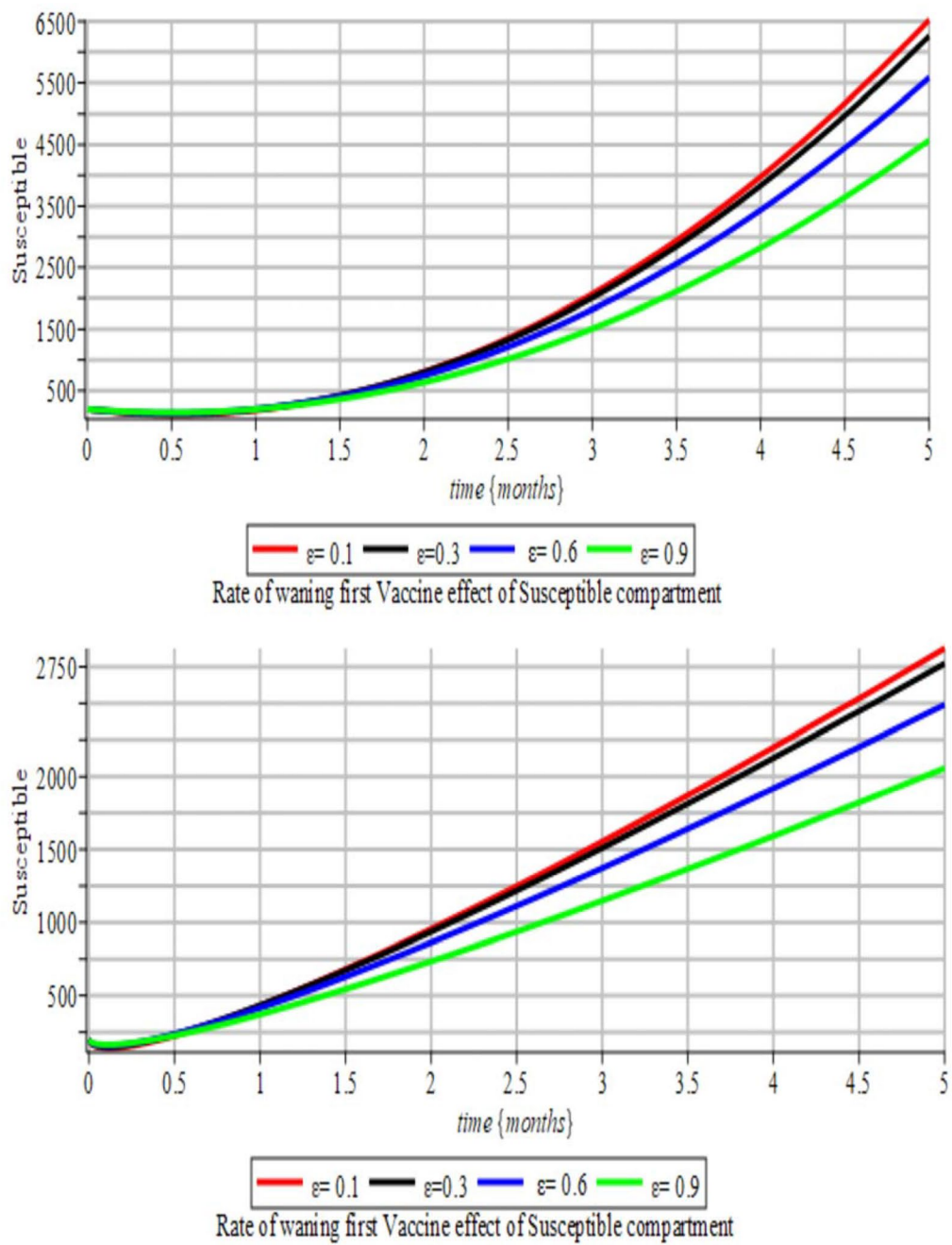


**Fig. 11** Effect of  $\epsilon$  on Classical and fractional

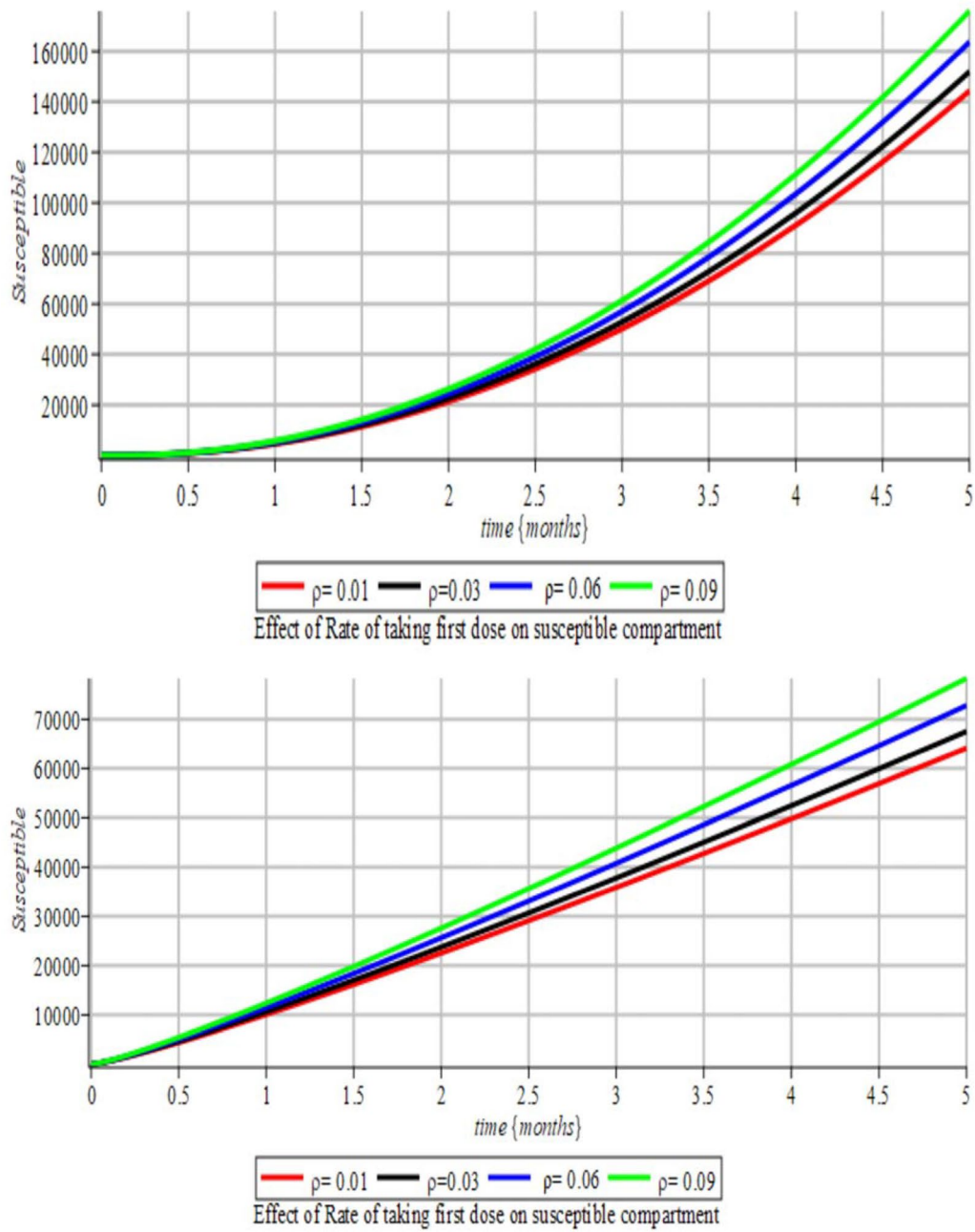


**Fig. 12** Effect of  $\rho$  on Classical and fractional

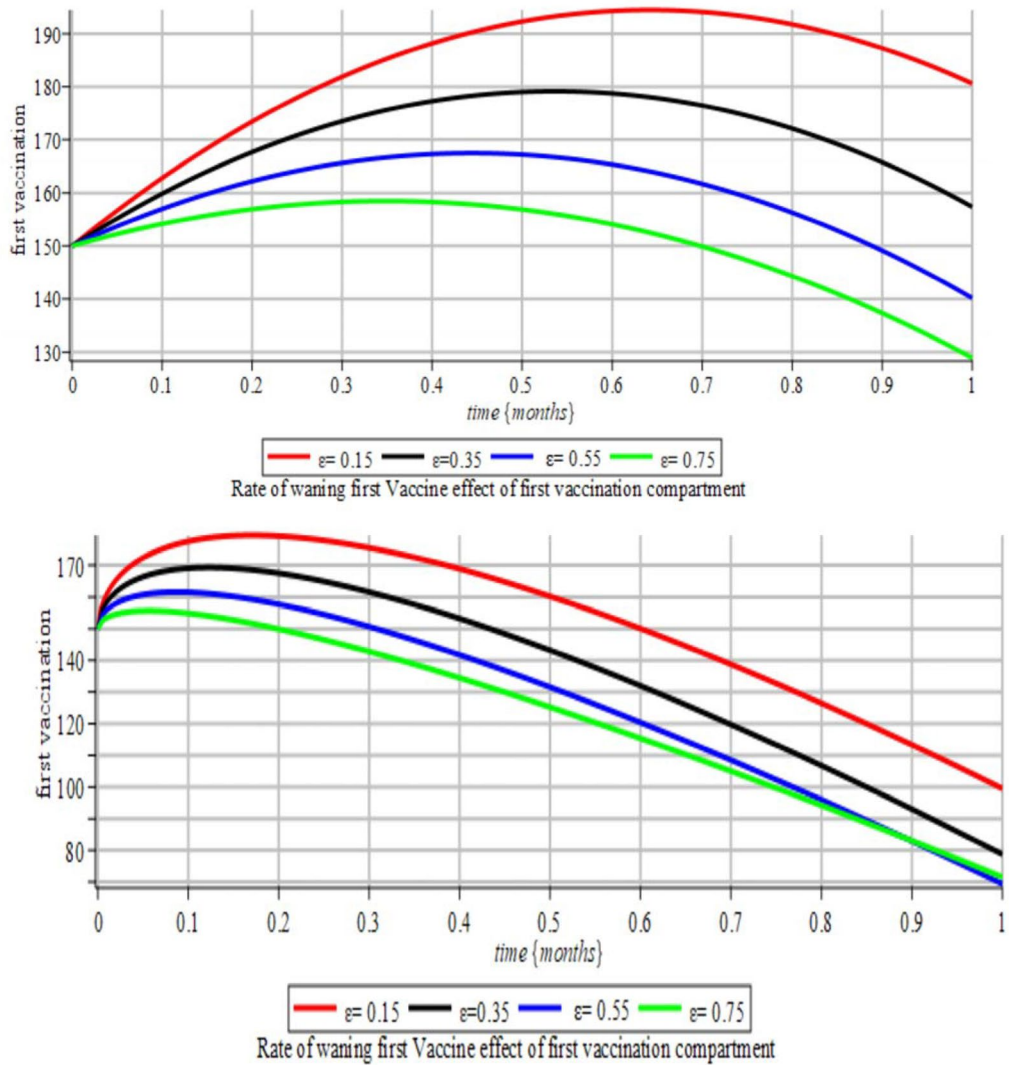


**Fig. 13** Effect of  $\epsilon$  on V1 Classical and fractional

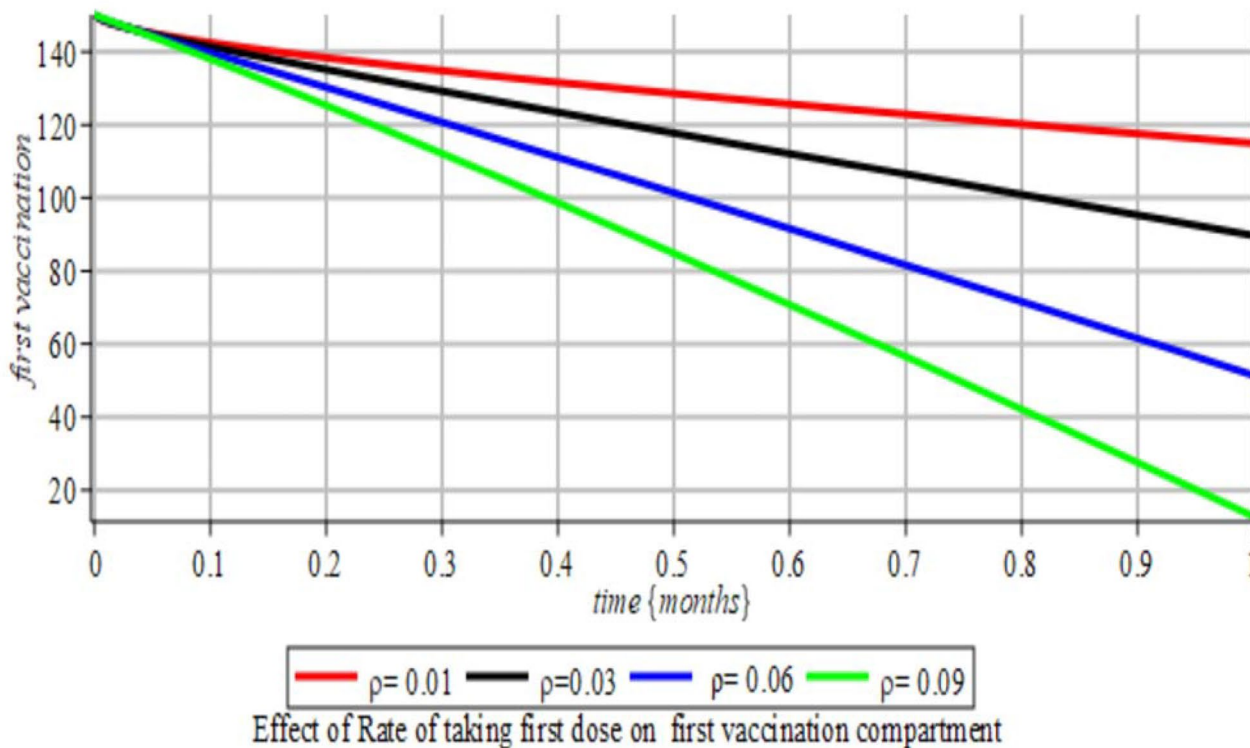
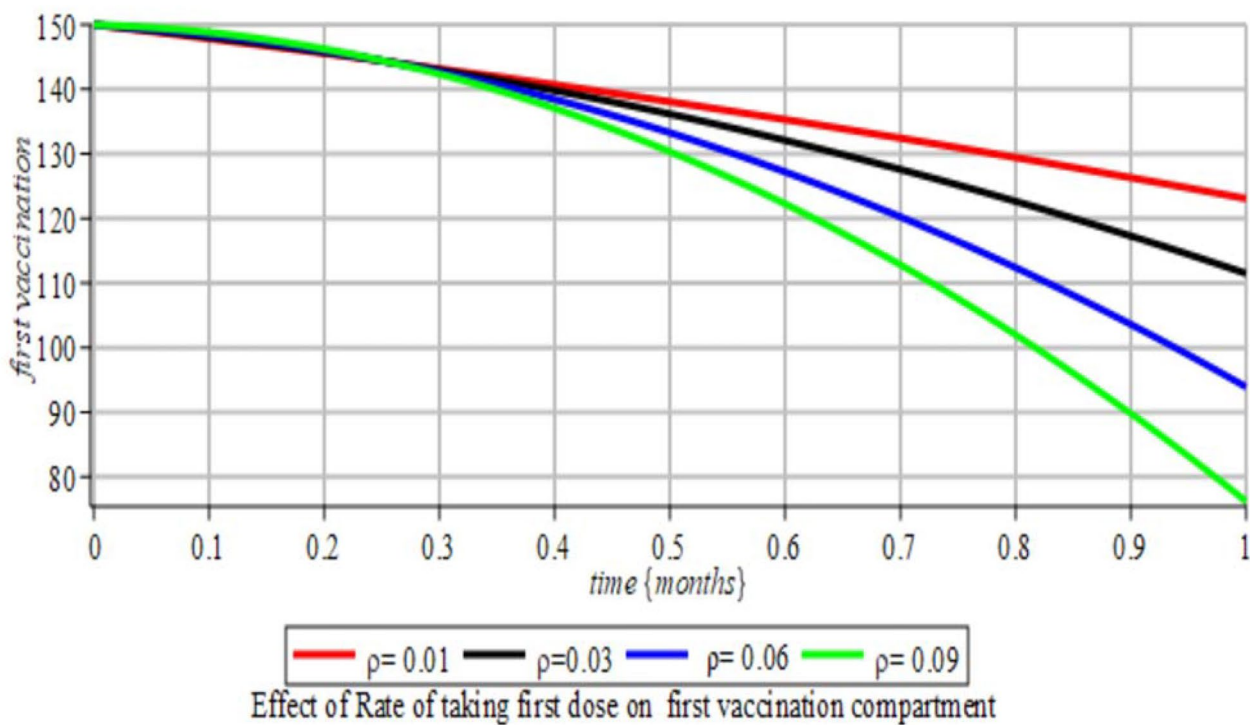


**Fig. 14** Effect of  $\rho$  on V1Classical and fractional

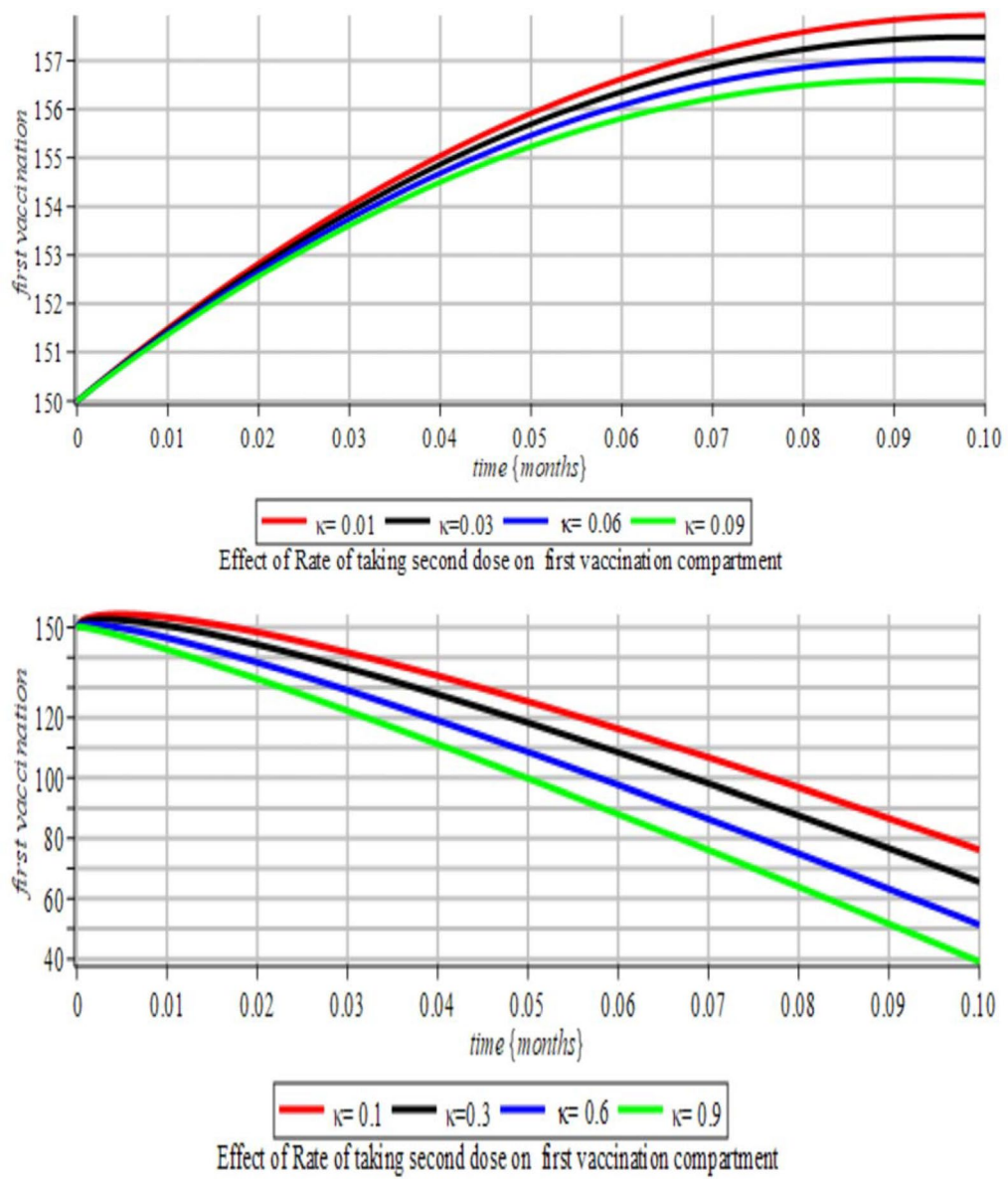


**Fig. 15** Effect of  $\kappa$  on V1Classical and fractional

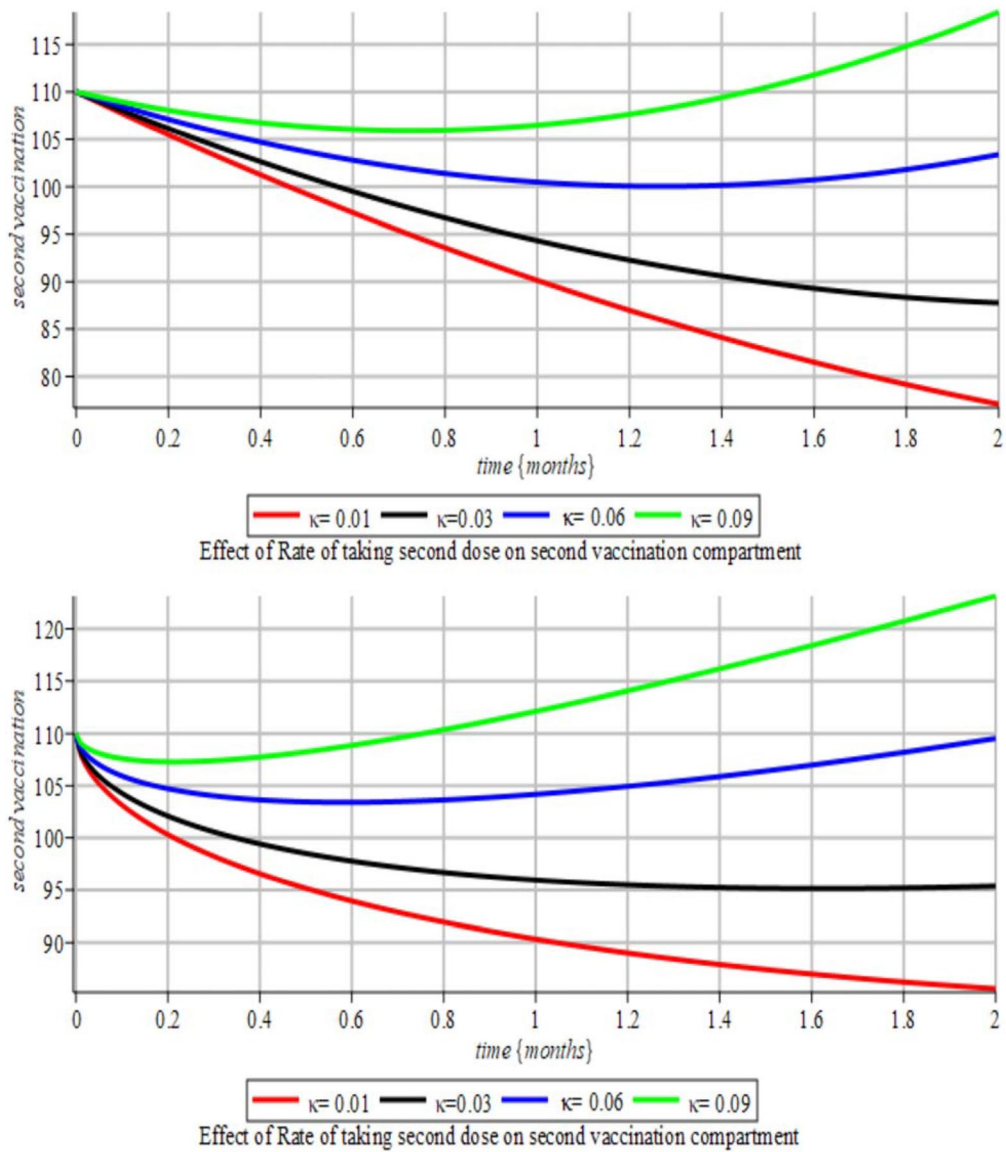
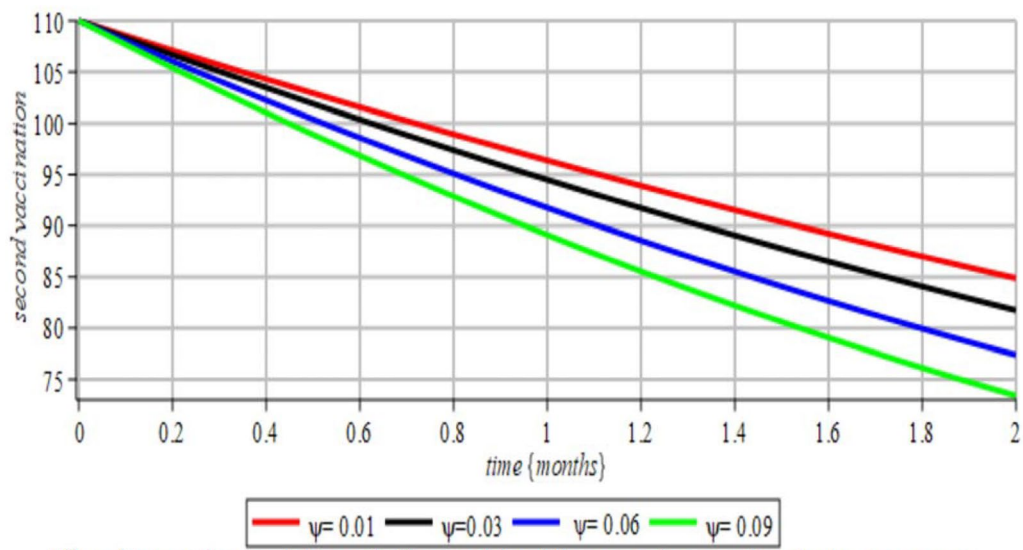
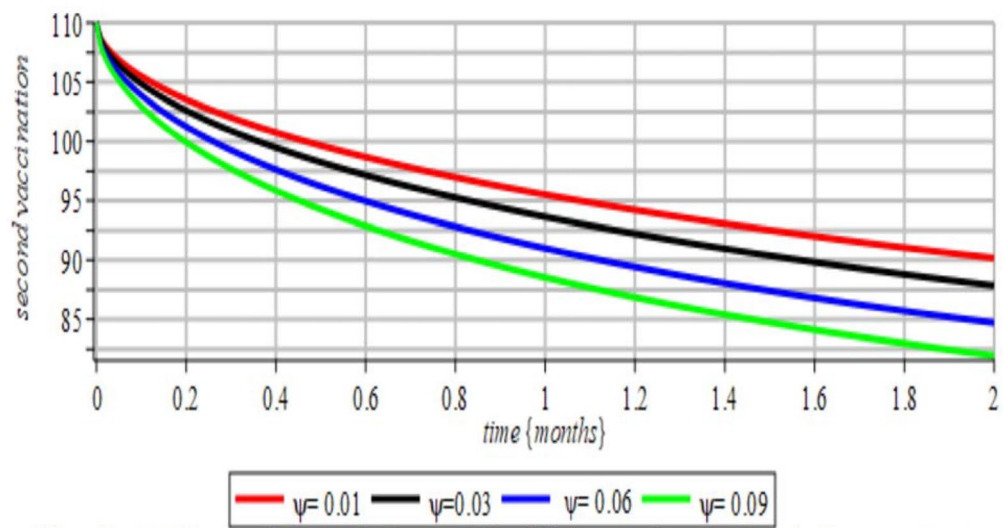


**Fig. 16** Effect of  $\kappa$  on V2 Classical and fractional



Effect of Rate at when people immured offer second dose fully recovered on second vaccination compartment



Effect of Rate at when people immured offer second dose fully recovered on second vaccination compartment

**Fig. 17** Effect of  $\psi$  on V2 Classical and fractional

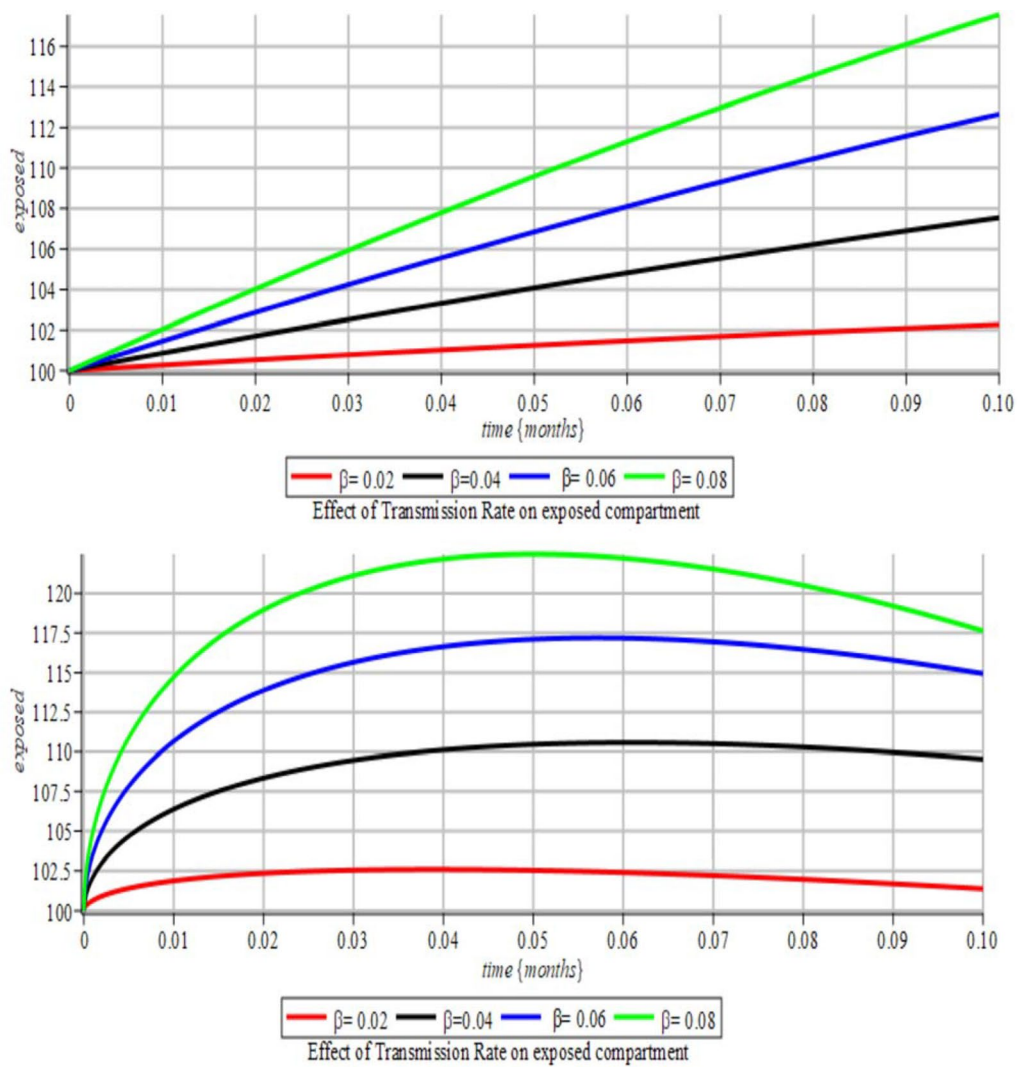


**Fig. 18** Effect of  $\beta$  on E Classical and fractional

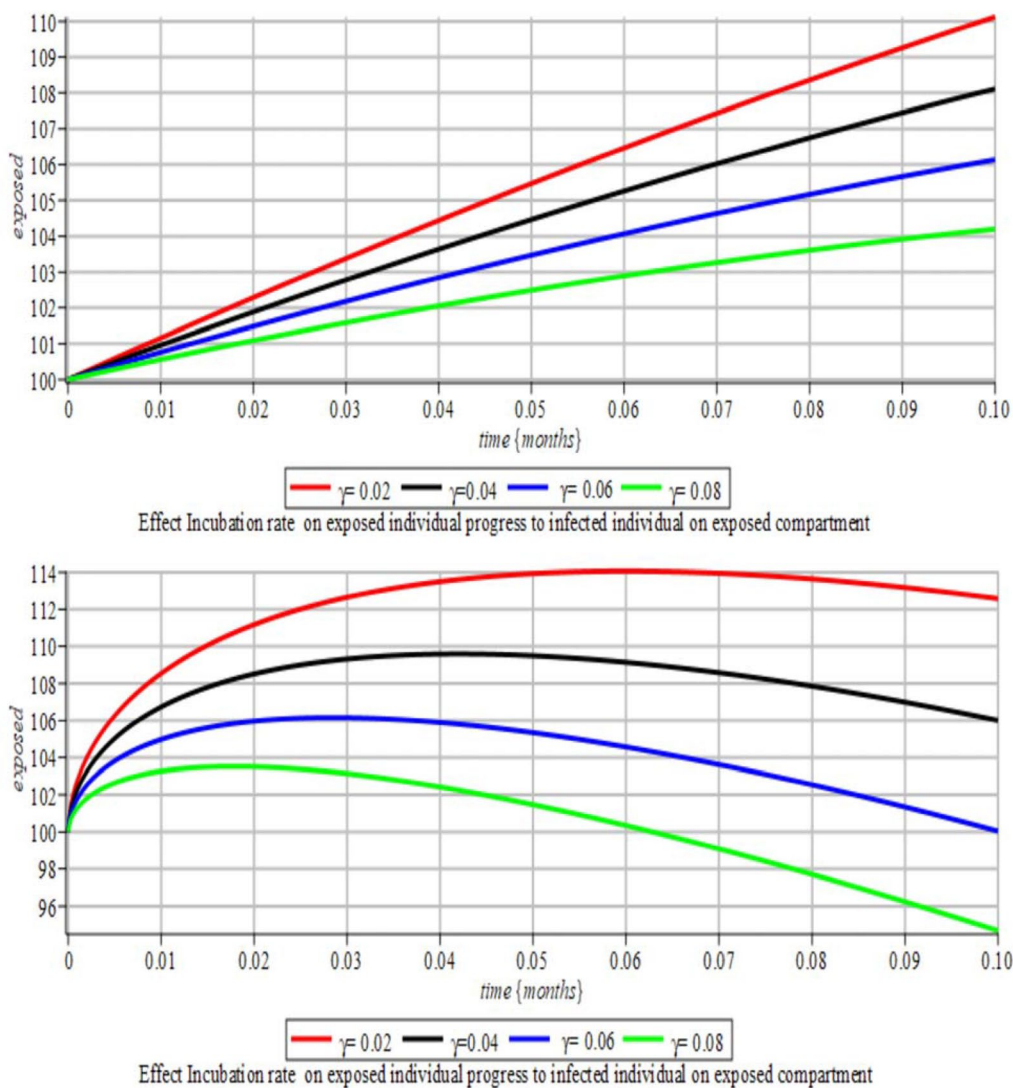


**Fig. 19** Effect of  $\gamma$  on  $E(t)$  Classical and fractional

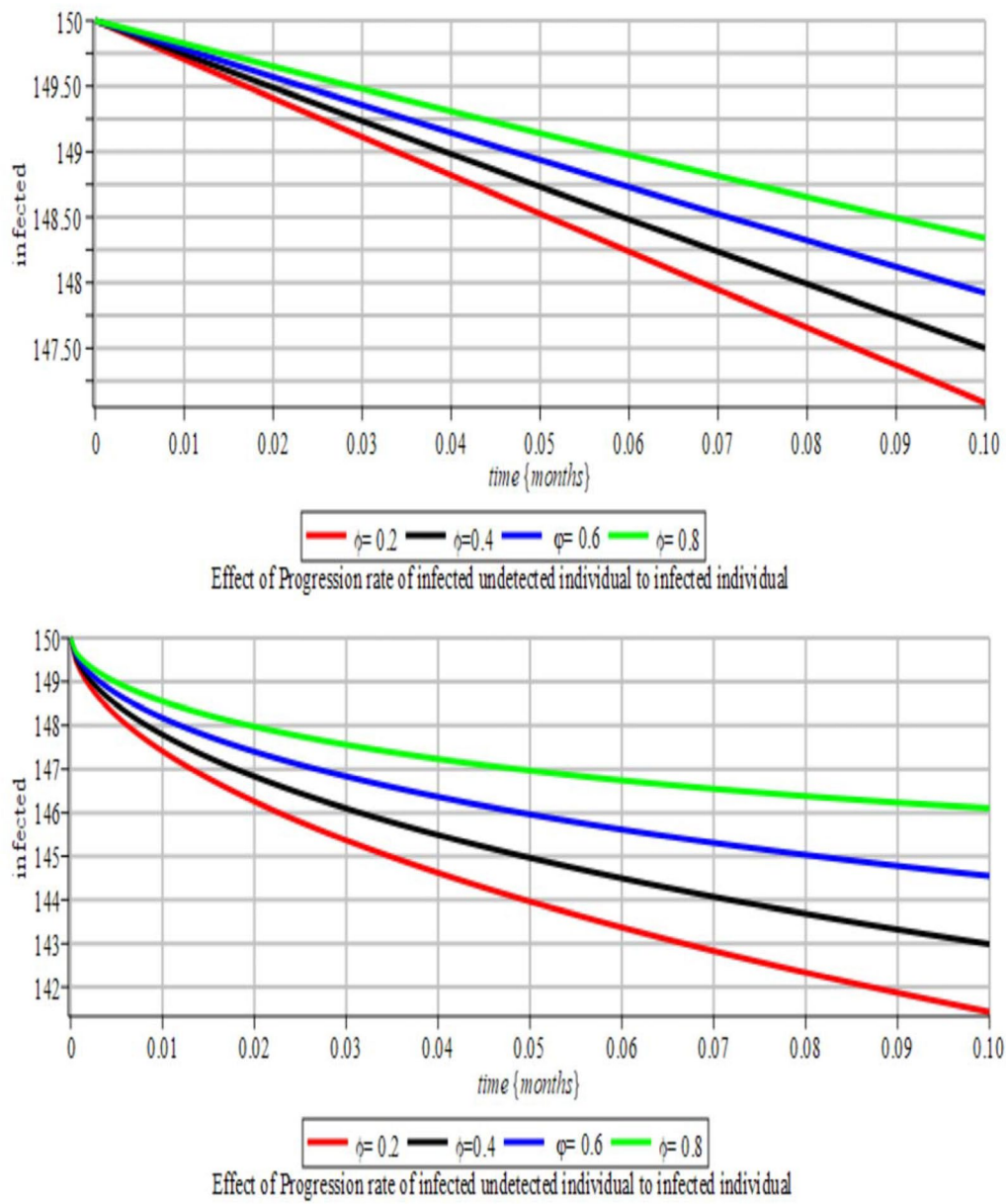


**Fig. 20** Effect of  $\phi$  on  $I(t)$ . Classical and fractional

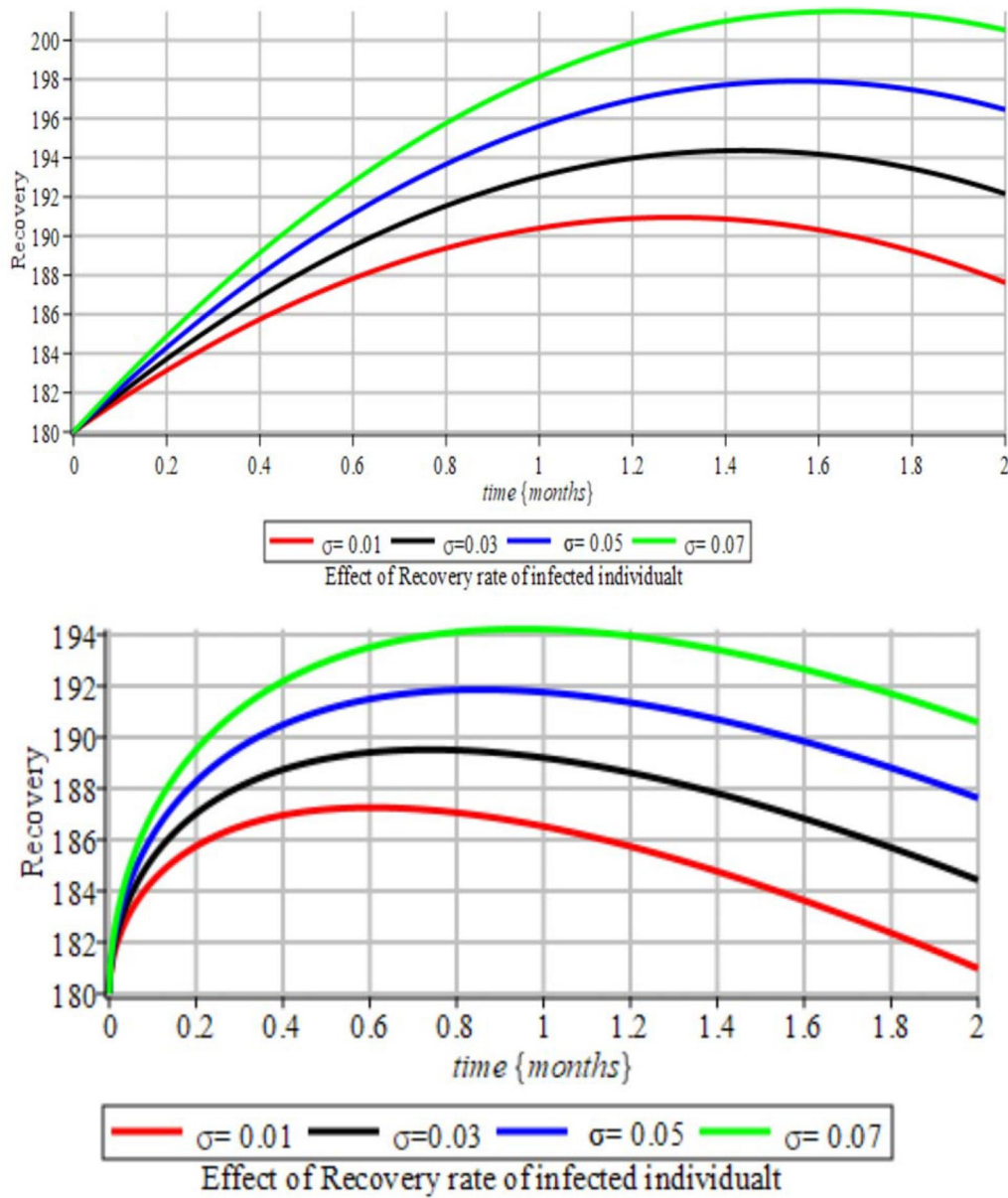


**Fig. 21** Effect of  $\sigma$  on  $R(t)$ . Classical and fractional

**Abbreviations**

LADM Laplace Adomian Decomposition Method  
 SAV1V2EUDTJR (Susceptible-First dose vaccination-Second dose vaccination-Exposed-Uninfected-Diagnosed-Treated-Isolated-Recovered)

**Acknowledgements**

The authors hereby acknowledge with thanks everyone who has contributed to the success of this research work.

**Author contributions**

Morufu O. Olayiwola: conceptualization, investigation, project administration, supervision, visualization, writing—review and editing. Akeem O. Yunus: formal analysis, writing—original draft, methodology, investigation, project administration, supervision, visualization, writing—original draft, writing—review and editing.

**Funding**

Not applicable.

**Availability of data and materials**

No datasets were generated or analysed during the current study.

**Declarations**

**Ethics approval and consent to participate**

Not applicable.

**Consent for publication**

Not applicable.

**Competing interests**

The authors declare no competing interests.

Received: 23 December 2024 Accepted: 31 March 2025

Published online: 30 April 2025

## References

- Yunus AO, Olayiwola MO, Adedokun KA, Adedeji JA, Alaje IA. Mathematical analysis of fractional-order Caputo's derivative of coronavirus disease model via Laplace Adomian decomposition method. *Beni-Suef Univ J Basic Appl Sci.* 2022. <https://doi.org/10.1186/s43088-022-00326-9>.
- Doohan P, Jorgensen D, Naidoo TM, McCain K, Hicks JT, McCabe R, Perez ZC. Lassa fever outbreaks, mathematical models, and disease parameters: a systematic review and meta-analysis. *Lancet Glob Health.* 2024;12(12):e1962–72.
- Almasaoudy R, Lopez JG, Rounds JA. Lassa Fever: from a Nigerian town to a global threat. 2023.
- Banda A, Gandiwa E, Muposhi VK, Muboko N. Ecological interactions, local people awareness and practices on rodent-borne diseases in Africa: a review. *Acta Trop.* 2022;238:106743.
- Olayiwola MO, Alaje AI, Olarewaju AY, Adedokun KA. A caputo fractional order epidemic model for evaluating the effectiveness of high-risk quarantine and vaccination strategies on the spread of COVID-19. *Healthc Anal.* 2023;3:100179.
- Aborode AT, Adesewa VA, Ayomide OE, Olarenwaju SO. Demanding of Lassa fever: reducing its risk as an infectious disease. *Health Sci J.* 2020;9:02.
- Enemuok NK, Obayi BA. Knowledge of Lassa fever disease and preventive measures among secondary school teachers in Enugu East Local Government Area. *Niger J Health Promot.* 2021;14(1):88–97.
- Ndenda JP, Njagarah JBH, Shaw S. Influence of environmental viral load, interpersonal contact and infected rodents on Lassa fever transmission dynamics: perspectives from fractional-order dynamic Modeling. *J AIMS Math.* 2022. <https://doi.org/10.3934/math.2022500>.
- Yunus AO, Omoloye MA. Mathematical analysis of efficacy of condom as a contraceptive on the transmission of chlamydia disease. *Int J Comput Sci Mobile Appl.* 2022. <https://doi.org/10.47760/ijcsma.2022.v10i02.002>.
- Olayiwola MO, Yunus AO. Non-integer time fractional-order mathematical model of the COVID-19 pandemic impacts on the societal and economic aspects of Nigeria. *Int J Appl Comput Math.* 2024;10(2):90.
- Yunus AO, Olayiwola MO. Mathematical modeling of malaria epidemic dynamics with enlightenment and therapy intervention using the Laplace-Adomian decomposition method and Caputo fractional order. *Franklin Open.* 2024;8:100147.
- Fichet-Calvet E, Becker-Ziija B, Koivogui L, Gunther S. Lassa serology in natural populations of rodents and horizontal transmission. *Vector Borne Zoonotic Dis.* 2014;14(9):665674.
- James TO, Abdulrahman S, Akinyesi S, Akinwade NI. Dynamics transmission of Lassa fever disease. *Int J Res Educ Sci.* 2015;2(1):2349–5219.
- World Health Organization. "Lassa fever: Factsheets". 2023. <https://www.who.int/mediacenter/factsheets/fs279/en/>. Accessed 24 Feb 2023.
- Li Y. Genetic basic underlying Lassa fever epidemics in the Mano River region, West Africa. *Virology.* 2023. <https://doi.org/10.1016/j.virol.2023.01.006>.
- Ali A, Ullah S, Khan MA. The impact of vaccination on the modeling of COVID-19 dynamics: a fractional order model. *Nonlinear Dyn.* 2022;110:3921–40. <https://doi.org/10.1007/s11071-022-07798-5>.
- Amer YA, Mashdy AMS, Shwayaa RT, Youssef ESM. Laplace transform method for solving nonlinear biochemical reaction model and nonlinear Emden Fowler system. *J Eng Appl Sci.* 2018;13(17):7388–94.
- Arqub OA, Al-Smadi M. Atangana-Baleanu fractional approach to the solutions of Bagley-Torvik and Painlevé equations in Hilbert space. *Chaos Solitons Fractals.* 2018;117:161–7.
- Yunus AO, Olayiwola MO. The analysis of a co-dynamic ebola and malaria transmission model using the Laplace Adomian decomposition method with Caputo fractional-order. *Tanzan J Sci.* 2024;50(2):224–43.
- Bakare EA, Are EB, Abolarin OE, Osanyinlusi SA, Ngwu B, Ubaka ON. Mathematical modelling and analysis of transmission dynamics of Lassa fever. *Hindawi J Appl Math.* 2022. <https://doi.org/10.1155/2020/6131708>.
- Nyenke C, Konne F, Ikpeama R. Updates on Lassa fever in Nigeria. *Healthc Issues.* 2022;1(1):1–8.
- Olayiwola MO, Yunus AO. Mathematical analysis of a within-host dengue virus dynamics model with adaptive immunity using Caputo fractional-order derivatives. *J Umm Al-Qura Univ Appl Sci.* 2024. <https://doi.org/10.1007/s43994-024-00151-z>.
- Yunus AO, Olayiwola MO, Omoloye MA, Oladapo AO. A fractional order model of Lassa disease using the Laplace-Adomian decomposition method. *Healthc Anal.* 2023;3:100167.
- Yunus AO, Olayiwola MO. The analysis of a novel COVID-19 model with the fractional-order incorporating the impact of the vaccination campaign in Nigeria via the Laplace-Adomian Decomposition Method. *J Niger Soc Phys Sci.* 2024;6:1830–1830.
- Abdullahi A. Modelling of transmission and control of Lassa fever via caputo fractional-order derivative. *Chaos Solitons Fractals J.* 2021;151:111271.
- Ben-Enukora CA, Adeyeye BK, Adesina E, Ajakaiye OOP, Adekanye O. Risk communication sources and knowledge of Lassa fever in Nigeria: an impact analysis. *NCNYON J.* 2022;8(11): e11335.
- Amakiri PC, Nkwoemeka NE, Okwelogu IS, Njoku OC, Chukwudi VN. Challenges to the control and eradication of Lassa fever virus in Nigeria. *Am J Public Health.* 2020;8(4):118–21.
- Gobir AA, Ejembi CL, Alhaji AA, Garba MB, Igboanus CJC, Usman B, Joshua IA. Knowledge of Lassa fever disease and its risk factors among rural people in a Nigerian Community. *Proceedings.* 2020;45(1):9.
- Izah SC, Iyiola AO, Poyeri WR, Ovuru KF. Lassa fever in Nigeria: case fatality ratio, social consequences, and prevention. In: Nazneen S, Abia ALK, Madhav S, editors. *Emerging pandemics.* Boca Raton: CRC Press; 2023. p. 133–50.
- Shen ZH, Chu YM, Khan MA, Muhammad S, Al-Hartomy OA, Higazy M. Mathematical modeling and optimal control of the COVID-19 dynamics. *Results Phys.* 2021;31:105028.
- Khan MA, DarAssi MH, Ahmad I, Seyam NM, Alzahrani E. Modeling the dynamics of tuberculosis with vaccination, treatment, and environmental impact: fractional order modeling. *CMES-Computer Model Eng Sci.* 2024;141(2):1365.
- Khan MA, DarAssi MH, Ahmad I, Seyam NM, Alzahrani E. The transmission dynamics of an infectious disease model in fractional derivative with vaccination under real data. *Comput Biol Med.* 2024;181:109069.
- Meetei MZ, DarAssi MH, Altaf Khan M, Koam AN, Alzahrani E, Ali H, Ahmadini A. Analysis and simulation study of the HIV/AIDS model using the real cases. *PLoS ONE.* 2024;19(6): e0304735.
- Oguntolu FA, Peter OJ, Yusuf A, Omede BI, Bolarin G, Ayoola TA. Mathematical model and analysis of the soil-transmitted helminth infections with optimal control. *Model Earth Syst Environ.* 2024;10(1):883–97.
- Peter OJ, Panigoro HS, Abidemi A, Ojo MM, Oguntolu FA. Mathematical model of COVID-19 pandemic with double dose vaccination. *Acta Biotheor.* 2023;71(2):9.
- Musa R, Peter OJ, Oguntolu FA. A non-linear differential equation model of COVID-19 and seasonal influenza co-infection dynamics under vaccination strategy and immunity waning. *Healthc Anal.* 2023;4:100240.
- Oshinubi K, Peter OJ, Addai E, Mwizerwa E, Babasola O, Nwabufor IV, Agbaje JO. Mathematical modelling of tuberculosis outbreak in an East African country incorporating vaccination and treatment. *Computation.* 2023;11(7):143.
- Omede BI, Peter OJ, Atokolo W, Bolaji B, Ayoola TA. A mathematical analysis of the two-strain tuberculosis model dynamics with exogenous re-infection. *Healthc Anal.* 2023;4:100266.
- Peter OJ, Madubueze CE, Ojo MM, Oguntolu FA, Ayoola TA. Modeling and optimal control of monkeypox with cost-effective strategies. *Model Earth Syst Environ.* 2023;9(2):1989–2007.

## Publisher's Note

Springer Nature remains neutral with regard to jurisdictional claims in published maps and institutional affiliations.